

Correlation of ignimbrites in the central Anatolian volcanic province using zircon and plagioclase ages and zircon compositions

Erkan Aydar ^{a,*}, Axel K. Schmitt ^{b,**}, H. Evren Çubukçu ^a, Lutfiye Akin ^a, Orkun Ersoy ^c, Erdal Sen ^a, Robert A. Duncan ^d, Gokhan Atici ^e

^a Hacettepe University Department of Geological Engineering, Beytepe, Ankara, 06800, Turkey

^b Department of Earth and Space Sciences, University of California, Los Angeles, 595 Charles Young Dr., Los Angeles, CA, 90095-1567, USA

^c Nigde University, Department of Geological Engineering, 51245 Nigde, Turkey

^d College of Oceanic and Atmospheric Sciences, Oregon State University, Corvallis, OR 97331, USA

^e General Directorate of MTA, Department of Geology, Dumlupinar Bulvarı, No: 139, 06800, Ankara, Turkey

ARTICLE INFO

Article history:

Received 26 June 2011

Accepted 10 November 2011

Available online 30 November 2011

Keywords:

Tephrostratigraphy

Pyroclastic deposits

Geochronology

Miocene

Continental plateau

ABSTRACT

Episodes of high eruptive fluxes ($> 10^{-3} \text{ km}^3/\text{year}$) in continental environments are associated with magmatism related to subduction, post-orogenic collapse, intra-plate hot spots, or rifting. During such episodes, voluminous ignimbrite deposits are produced which cover landscapes over 10^4 – 10^5 km^2 . In such sequences, brief eruptive recurrence and chemical similarity limit the applicability of geochronological and geochemical correlation methods. Here, we present complementary geochronological data ($^{40}\text{Ar}/^{39}\text{Ar}$ plagioclase eruption and $^{206}\text{Pb}/^{238}\text{U}$ zircon crystallization ages) for ignimbrites from the Miocene–Holocene Central Anatolian Volcanic Province (CAVP). In addition, we successfully employed zircon geochemistry (trace elements, oxygen isotopes) as an alteration-resistant indicator to correlate rhyodacitic to rhyolitic ignimbrites whose eruption age differences are too brief to be resolved by $^{40}\text{Ar}/^{39}\text{Ar}$ geochronology. By applying this method, we dismiss previous correlations between stratigraphic members (i.e., Sofular and Gördeles, Sofular and Sarımadentepe), but demonstrate close relationships for other CAVP ignimbrites (i.e., Kavak units 1 to 4; Cemilköy ignimbrite and overlying fallout deposits). Our chronostratigraphy reveals two previously unrecognized eruptive pulses at ~ 9 – 8 Ma and 7 – 5 Ma which are characterized by increasing magmatic temperatures (~ 75 – $100 \text{ }^\circ\text{C}$ within each cycle). Despite a long-term (10 Ma) eruptive productivity that is about one order of magnitude smaller than in other magmatically active continental plateaus, the CAVP achieved high eruptive fluxes during brief (1–2 Ma) intervals.

© 2011 Elsevier B.V. All rights reserved.

1. Introduction

Extensive pyroclastic flow deposits (ignimbrites) are generated by ground-hugging pyroclastic density currents that result from eruption of volatile-rich dacitic to rhyolitic magmas at high discharge rates (Smith, 1960; Wilson et al., 1980). The resulting deposits, frequently erupted from calderas, form extensive volcanic provinces in many locations worldwide (e.g., Western North America; Central Andes, North Island of New Zealand, Central Anatolia) where subduction (fluid-fluxed) and post-collisional, hot-spot, or rift-related (decompression) mantle-derived magmatism has imprinted on continental crust (e.g.,

De Silva, 1989; Perry et al., 1993; McCulloch et al., 1994; Temel et al., 1998; Ferrari et al., 2002; Bryan and Ernst, 2008). In these provinces, pyroclastic fallout deposits can be widely and coherently dispersed forming prominent marker beds (e.g., Wilson et al., 1995), and individual pyroclastic flows can travel large distances ($\sim 100 \text{ km}$; Wörner et al., 2000). Because of flow channelization, thickness and distribution of ignimbrites vary locally which impedes lateral correlation by mapping, especially in older, more eroded sequences. Moreover, mineralogical and chemical homogeneity of ignimbrites within individual provinces, alteration of poorly indurated glassy rocks, and an abundance of accidental lithic and crystal components can frustrate correlation using conventional geochronological and geochemical tools (e.g., Hildreth and Mahood, 1985; Glazner et al., 1986; De Silva, 1989; Shane, 1998).

In the Central Anatolian Volcanic Province (CAVP), Miocene–Pliocene ignimbrites collectively cover $20,000 \text{ km}^2$ (Le Pennec et al., 1994). This estimate extrapolates over in part deeply incised erosional remnants of these ignimbrites. These deposits, intercalated with terrestrial sediments and local lava flows, form a bizarre badlands-type landscape. Despite multi-decadal research, the stratigraphic relations within the CAVP

* Corresponding author. Tel.: +90 312 297 77 07; fax: +90 312 299 20 34.

** Corresponding author. Tel.: +1 310 206 5760; fax: +1 310 825 2779.

E-mail addresses: eaydar@hacettepe.edu.tr (E. Aydar), axel@oro.ess.ucla.edu (A.K. Schmitt), ecubukcu@hacettepe.edu.tr (H.E. Çubukçu), lutfiye_akin@hacettepe.edu.tr (L. Akin), oersoy@nigde.edu.tr (O. Ersoy), erdals@hacettepe.edu.tr (E. Sen), rduncan@coas.oregonstate.edu (R.A. Duncan), gokhana@mta.gov.tr (G. Atici).

have remained controversial because of difficulties in laterally tracing individual ignimbrites, and geochronological data (mostly based on K–Ar whole-rock analyses, due to the absence of sanidine) that frequently is problematic because of unconstrained parent–daughter isotopic disturbance (Pasquarè, 1968; Le Pennec et al., 1994; Mues-Schumacher and Schumacher, 1996; Le Pennec et al., 2005; Viereck-Götte et al., 2010). Similar complications, such as the scarcity or absence of sanidine, affect stratigraphic correlations in other continental ignimbrite provinces such as the Altiplano Puna and the Sierra Madre Occidental (e.g., McDowell, 2007; Salisbury et al., 2011).

To overcome these limitations, we employ zircon as a robust chronometer and indicator mineral that is unaffected by alteration, and combine it with $^{40}\text{Ar}/^{39}\text{Ar}$ stepwise-heating of plagioclase. This permits a consistency check for disturbance of the parent–daughter relations in the K–Ar decay system because zircon reliably dates crystallization in a magma and is unaffected by post-magmatic heating or alteration. However, zircon frequently displays significant pre-eruptive residence or recycling. Such crystals have been termed antecrysts (see reviews in Simon et al., 2008; Schmitt, 2011), and because of their ubiquity in silicic magmas, zircon strictly provides a maximum age for the eruption. $^{40}\text{Ar}/^{39}\text{Ar}$ dating, by contrast, can yield reliable eruption ages, but the K–Ar decay system in materials available for dating in CAVP ignimbrites (e.g., plagioclase, biotite, glass) can be more readily disturbed than zircon (e.g., by excess ^{40}Ar , or K mobility; Cerling et al., 1985; Hora et al., 2010), or affected by xenocrytic contamination (e.g., Spell et al., 2001). It is therefore advantageous to combine zircon and plagioclase, ages which – if concordant – can collectively establish a robust chronostratigraphic framework. For key CAVP ignimbrites dated here, only a few cases revealed complex crystal origins for zircon. Trace elements and oxygen isotopes in zircon further allow for correlation between units where eruption and crystallization age uncertainties overlap. This highlights the potential of zircon as a reliable indicator mineral for the correlation of ignimbrites.

2. Geological background

2.1. Outlines of Central Anatolian Volcanism

Central Anatolia constitutes a high plateau at 1400–1500 m elevation which hosts a continental volcanic province with eruptions of Miocene to Upper Holocene age (here termed Central Anatolian Volcanic Province CAVP; Fig. 1). This province is also known under its regional name Cappadocia (etymologically: “the land of beautiful horses”), and several other names have been used in the literature (Central or Centro-Anatolian Plateau, Anatolian Highland, Ürgüp plateau, Neogene plateau in Pasquarè, 1968, or Nevşehir Plateau in Le Pennec et al., 1994). Topographically a gently N-dipping depression, it is bounded by the Taurus Mountain range in the south, and two prominent Quaternary stratovolcanoes (Hasan Dag and Erciyes Dag) in the west and east, respectively. Neogene continental sediments, mostly endorheic fluvial and lacustrine deposits, and late-orogenic volcanic deposits (Pasquarè, 1968) fill this depression. Structurally, the western and eastern limits of the plateau are defined by the Tuzgölü and Eçemis faults, respectively (Fig. 1).

Numerous studies have addressed various volcanological, petrological, geochemical, and tectonic aspects of the CAVP (e.g., Beekman, 1966; Pasquarè, 1968; Innocenti et al., 1975; Besang et al., 1977; Pasquarè et al., 1988; Schumacher et al., 1990; Temel, 1992; Le Pennec et al., 1994; Toprak et al., 1994; Aydar et al., 1995; Druitt et al., 1995; Notsu et al., 1995; Mues-Schumacher and Schumacher, 1996; Schumacher and Mues-Schumacher, 1996; Schumacher and Mues-Schumacher, 1997; Aydar and Gourgaud, 1998; Temel et al., 1998; Şen et al., 2003; Le Pennec et al., 2005; Viereck-Götte et al., 2010; Schmitt et al., 2011). Apart from its landmark ignimbrites, the CAVP comprises eroded Miocene andesitic volcanic complexes, as well as lava fields and flows (e.g., Aydar and Gourgaud, 1998). In addition, several

Quaternary stratovolcanoes (such as Erciyes Dag, Hasan Dag) and numerous monogenetic vents (cinder cones, maars, domes) exist (Aydar and Gourgaud, 1998). Stratigraphically, the Ürgüp formation (Pasquarè, 1968) is the major lithostratigraphic unit which was originally subdivided into nine ignimbrite members (lentils or tongues if discontinuous; Fig. 2; Table 1): Akkoy, Kavak, Sarımaden Tepe Tongue, Cemilköy, Tahar, Gördeles, Incesu Member, Sofular Lentil, and Valibabatepe, so named after type localities (villages and hills, for which the Turkish names are “köy” and “tepe”, respectively). The voluminous rhyolitic–dacitic ignimbrites are separated by fluvio-lacustrine sediments, soil, or lava flows (Fig. 3). Besides mammalian biostratigraphy and magnetostratigraphy (Pasquarè, 1968; Le Pennec et al., 2005), only limited radiometric (K/Ar) data has been available for the CAVP (e.g., Innocenti et al., 1975; Mues-Schumacher and Schumacher, 1996).

2.2. Comparative stratigraphies

Cretaceous granitic and gabbroic rocks constitute the pre-volcanic basement of Cappadocia with outcrops mainly in the Acıgöl, Tilköy, and Keslik area. This is confirmed by ages for a granitic sample from the Acıgöl area ($^{40}\text{Ar}/^{39}\text{Ar}$ age: 78.4 ± 0.4 Ma; $^{206}\text{Pb}/^{238}\text{U}$ zircon age: 77.8 ± 4.4 Ma; Tables 1 and 2). Outside the CAVP, the substratum comprises metamorphic rocks of the Central Anatolian Crystalline Complex (Dilek and Sandvol, 2009). Pre-volcanic rocks such as the Yesilhisar conglomerates frequently form xenolithic fragments in CAVP pyroclastic rocks.

In our stratigraphic re-evaluation of the CAVP (Table 1; Figs. 2 and 3; see also map in electronic Appendix 1), we follow the terminology outlined in Le Pennec et al. (1994), identifying 10 ignimbrite members (in stratigraphic order from old to young): Kavak, Zelve, Sarımadentepe, Sofular, Cemilköy, Tahar, Gördeles, Kızılkaya, Valibabatepe, and Kumtepe (Table 1).

2.3. Kavak ignimbrite

The Kavak ignimbrites represent the oldest pyroclastic deposits in the CAVP. They are interbedded with fluvio-lacustrine sediments indicating multiple eruptive episodes (stratigraphic column in electronic Appendix 2). Collectively, the Kavak ignimbrites have a volume of $\sim 80 \text{ km}^3$ distributed over a $\sim 2600 \text{ km}^2$ area (Le Pennec et al., 1994). Mues-Schumacher and Schumacher (1996) and Le Pennec et al. (2005) subdivided the Kavak ignimbrites into multiple sub-units separated by sediments (e.g., Upper and Lower Göreme ignimbrites; Table 1). Lately, Viereck-Götte et al. (2010) proposed two new ignimbrite members underlying the Lower Göreme: Guvercinlik and Eneski. Here, we maintain a collective term for all Kavak ignimbrites because of their temporal and lithological similarity, and a lack of mappable marker horizons.

Kavak ignimbrites are well exposed in the eastern and northeastern parts of the Çardak depression which is their probable source area (Froger et al., 1998). The sequence (electronic Appendix 2) starts with a whitish ashy fallout deposit followed by a reversely graded pumice-rich flow (Kavak-1). Ash-rich lacustrine sediments separate the Kavak-1 subunit from overlying Kavak-2. The Kavak-2 subunit has a base rich in andesitic lithics, which diminish in abundance up-section and grade into ash-rich flow deposits near the top. Characteristic accretionary lapilli are present north-northeast of Kavak village and in the Nar valley. Carbonaceous fluvio-lacustrine conglomerates with a small intercalated pumiceous fallout deposit separate Kavak-2 from Kavak-3. Kavak-3 is consolidated to moderately indurated with several pumice-rich horizons in an ash matrix and overlain by ~ 50 cm of yellowish-beige pumiceous fallout of Kavak-4. This unit is characteristically pale pinkish in color and its overlying pyroclastic flow deposit contains few lithic and pumice clasts in an ash-rich matrix. The top of the sequence comprises intensely weathered ash fallout deposits with dark-gray to black altered pumice.

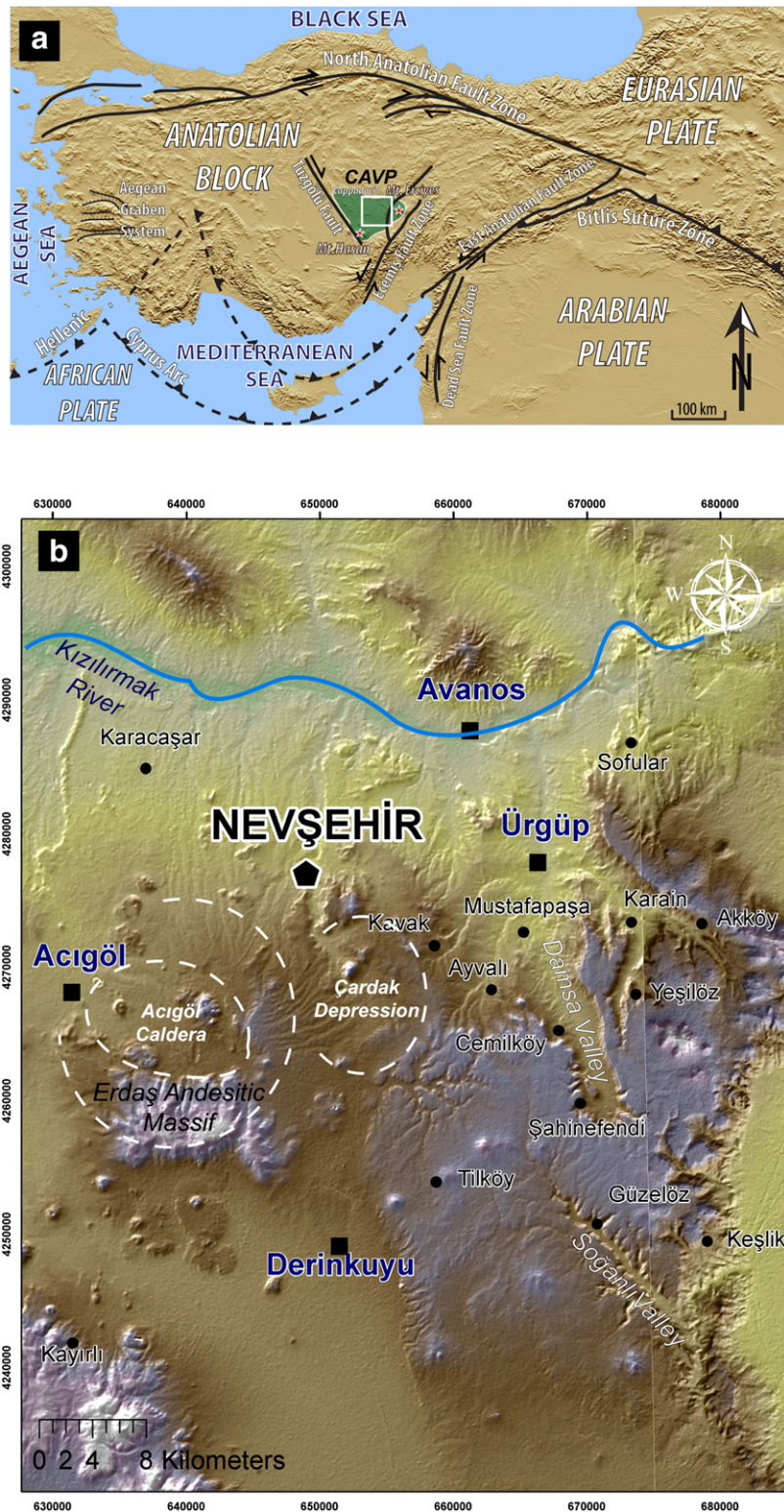


Fig. 1. (a) Overview map of the Central Anatolian Volcanic Province (CAVP) including prominent tectonic structures in Anatolia. (b) Digital elevation model of the study area (inset in panel a) showing major eruptive centers for CAVP ignimbrites.

All Kavak ignimbrites contain crystal-rich pumice with large (3 to 5 mm) phenocrysts of biotite, plagioclase, and quartz. Alkali feldspar is absent (cf. Le Pennec et al., 1994). Intense devitrification and alteration are common. We could not confirm the presence of carbonized plants (cf. Le Pennec et al., 1994) but subaerial emplacement

conditions are indicated by our discovery of well-preserved *rhinocerotidae* skull and bones (upper and lower jaws, femurs; S. Sen, pers. comm.) in the Kavak-4 deposit near Karacaşar (north-eastern Acıgöl). The good preservation of the bones implies low-temperature emplacement in a subaerial environment.

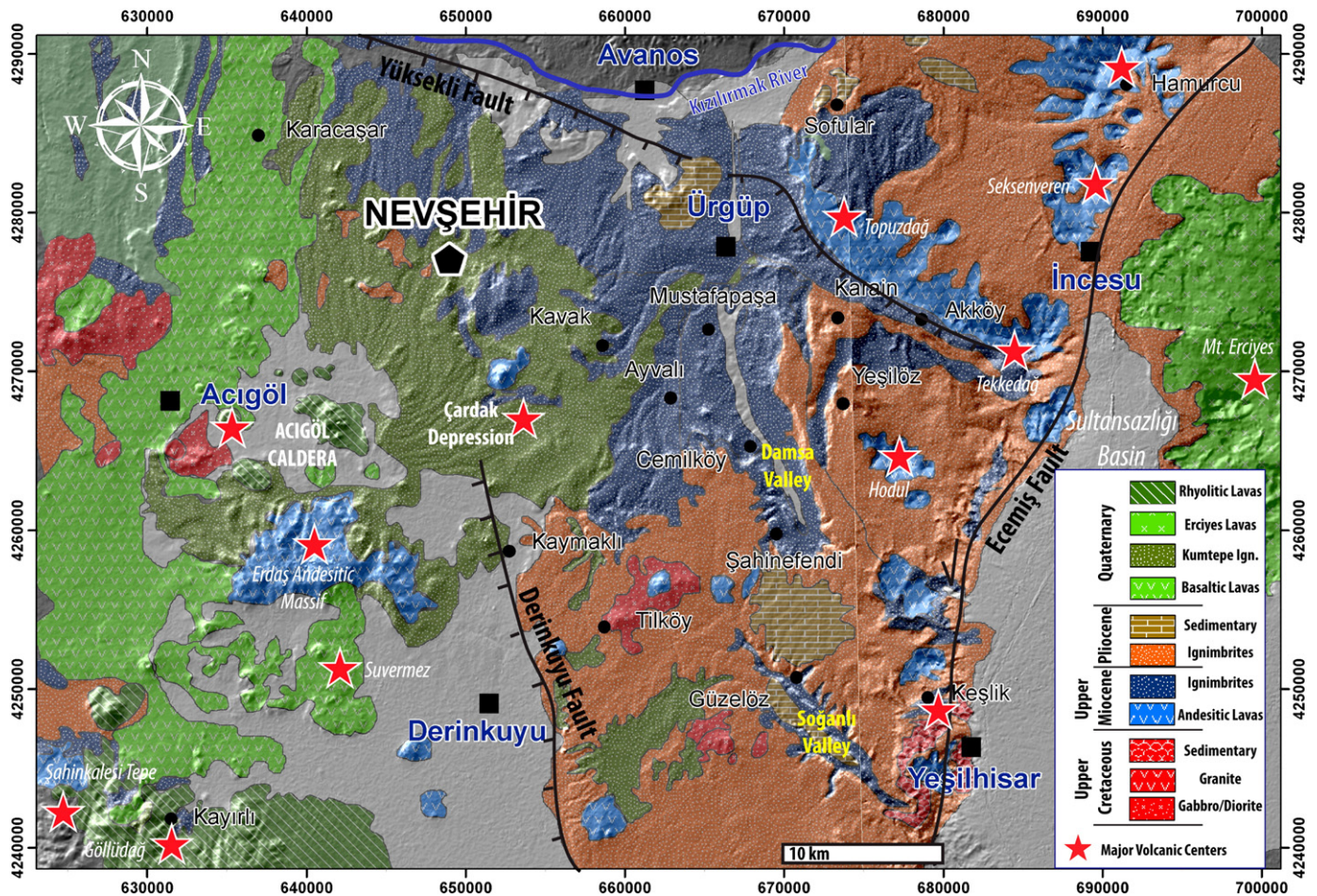


Fig. 2. Generalized geologic map of the CAVP with distributions of Miocene (Kavak, Zelve, Sofular, Sarımadentepe, Cemilköy, Tahar, and Gördeles), Pliocene (Kızılkaya and Valıbabatepe) and Quaternary (Kumtepe) ignimbrite units and major volcanic centers. For clarity, units are undifferentiated within each age group, and interbedded fluvio-lacustrine sediments have been omitted.

2.4. Zelve ignimbrite

Zelve ignimbrite is one of the most spectacular ignimbrites of Cappadocia where it is frequently quarried as masonry stone. It shows a snow-white basal pyroclastic fallout deposit overlain by a single cooling unit of indurated pink ignimbrite (stratigraphic column in electronic Appendix 3). It likely originated from a source near to that of the Kavak ignimbrites and covers $\sim 4200 \text{ km}^2$ around Ürgüp, Avanos, and Nevşehir with a total volume of $\sim 120 \text{ km}^3$ (Le Pennec et al., 1994).

In detail, the Zelve ignimbrite consists of two distinct eruptive deposits: rhyolitic pumice fallout up to 10 m thick and partly interbedded with pyroclastic surges (Schumacher and Mues-Schumacher, 1997) and an overlying single-cooling-unit ignimbrite. Pumice in the basal fallout is glassy and tubular with scarce phenocrysts of plagioclase, biotite, and quartz. Devitrification and alteration occasionally replace pumice glass with yellowish zeolitic aggregates. Overlying the basal fallout is a series of pyroclastic units which display laminated, plane-parallel, or low-angle cross bedding. The three major divisions are (in stratigraphic order): the lower surge series, the upper pumice beds, and the upper surge series (Schumacher and Mues-Schumacher, 1997). Accretionary lapilli are abundant in these deposits and were characterized as both, rim-type (Schumacher and Schmincke, 1991; Schumacher and Mues-Schumacher, 1997) and core-type in a pumice layer in the upper surge series (Schumacher and Schmincke, 1991). At variance with Le Pennec et al. (1994) are observations by Schumacher

and Mues-Schumacher (1997) and us that accretionary lapilli also occur within in the basal fall-out as well as the overlying flow deposits, indicating water–magma interaction throughout the eruption sequence.

The main ignimbrite body is typically beige to pink, with gradation from pumice-rich to ash-rich and lithic-poor in the middle parts of the section. Rhythmic inverse grading of pumice exists in multiple flow units towards the top of the section, with interspersed lithic-rich horizons and occasional accretionary or armored lapilli (Le Pennec et al., 1994; Schumacher and Mues-Schumacher, 1997). Locally, sub-spherical barite concretions exist whose abundance appears to be related to faults, indicative of localized hydrothermal activity. The Zelve ignimbrite also exhibits secondary alteration of volcanic glass into erionite-, clinoptilolite-, and chabasite-type zeolites around Sarıhıdır and Tuzköy villages where the ignimbrite potentially entered a lake.

2.5. Sarımadentepe ignimbrite

The Sarımadentepe ignimbrite has scattered exposures in the Nevşehir Plateau with varying estimates for area (3900 and 5200 km^2) and volume (80 and 110 km^3) in Le Pennec et al. (1994) and Viereck-Götte et al. (2010), respectively. Our field work supported by whole-rock geochemical correlation suggests a much smaller size of the Sarımadentepe ignimbrite. It is exclusively localized in the eastern to southeastern part of the Çardak depression (Mustafapaşa and Ayvalı

Table 1
Published and new stratigraphic relations for CAVP ignimbrites.

Beekman, 1966	Pasquarè, 1968	Innocenti et al., 1975	Besang et al., 1977	Temel, 1992	Le Pennec et al. 1994	Schumacher et al., 1990	Schumacher and Schumacher, 1996	Le Pennec et al., 2005	Viereck-Coette et al., 2010	This study
	Vallibabatepe	Vallibabatepe 2.7±0.1 2.8±0.1 3.0±0.1			Vallibabatepe	Vallibabatepe Incesu	Vallibabatepe-Sofular 1.1±0.1 2.8±0.1	Vallibabatepe 2.6-3.0	Incesu member	Kumtepe lgn. Valibabatepe lgn. 2.52±0.49
	Sofular	Andesite (5Ma) Karahoyuk 4.4±0.1								
Kizilkaya	Incesu	Baskoy 5.4±1.1	Kizilkaya 4.9±0.2 5.5±0.2		Kizilkaya	Kizilkaya	Kizilkaya 4.3±0.2 4.3±0.2 4.5±0.2	Kizilkaya 4.5-5.5	Kizilkaya member	Kizilkaya lgn. 5.19±0.07 5.11±0.37
	Gordeles	Sofular 6.8±1.4			Gordeles	Gordeles	Gordeles 4.0±0.2	Gordeles 6.8-7.6	Gordeles member	Gordeles lgn. 6.34±0.07 6.33±0.23
	Tahar	Gordeles 7.8±1.6			Tahar	Tahar	Tahar 6.5±0.2 6.8±0.2	Tahar 7.2-7.8	Tahar member	Tahar lgn. 6.14±0.22 6.07±0.67
Selime Tuff	Cemilkoy				Cemilkoy	Cemilkoy	Cemilkoy 6.5±0.2 6.8±0.2	Cemilkoy 7.6-8.4	Cemilkoy member	Cemilkoy lgn. 7.20±0.09 6.66±0.40
Gostuk	Sanmadentepe	Sarimdentepete 8.0±1.6 8.2±1.6			Sarimadentepe	Sarimadentepe	Sarimadentepe	Sarimadentepe 8.05-8.7	Sarimaden Tepe member	Sofular lgn. Sarmaden Tepe lgn. 8.44±0.12 8.59±0.51
	Kavak	Kavak 8.6±1.7		Kavak 11.2±2.5	Zelve	Akdag	Akdag-Zelve 7.5±0.2 7.7±0.2 6.9±0.2	Zelve 8.5-9.0	Zelve member	Zelve lgn. 9.19±0.15 9.13±0.40
	Akkoy	Akkoy 8.5±0.2			Kavak	Upper Goreme Lower Goreme	Upper Goreme 9.2±0.2	Kavak 9.0-14	Kavak member	Kavak lgn. 9.20±0.10 9.43±0.38 AFD:5108±0.06 AFD:1009±0.5
									Lower and Upper Goreme Bed Lower and Upper Uchisar Beds	
									Güvercinlik member	
									Ereski member	

EPOCH		LITHOLOGY	DEFINITION	Ar/Ar Age (Ma)	U-Pb Zircon Age (Ma)
Pleistocene			Acıgöl Rhyolites Acıgöl Basalt		
			Kumtepe Ign.		
Pliocene			Göllüdağ Rhyolites Basalts		
			Valibabatepe Ign.	2.52±0.49	
UPPER MIOCENE	UNITS		Kışladağ Limestone (Derinkuyu Andesite)		
			Kızılkaya Ign.	5.19±0.07	5.11±0.37
			Hodul Lavas Fluvio-Lacustrine Sediments		
			Gördeles Ign.	6.34±0.07	6.33±0.23
			Fluvio-Lacustrine Sediments		
			Tahar Ign.	6.14±0.22	6.07±0.67
			Fluvio-Lacustrine Sediments		
			*Air fall Deposit		
			Fluvio-Lacustrine Sediments		
			Cemilköy Ign.	7.20±0.09	6.66±0.40
			Fluvio-Lacustrine Sediments		
			Topuzdağ Lavas Fluvio-Lacustrine Sediments		
			Sofular Ign.	8.17±0.08	8.32±0.37
			Sarımadentepe Ign.	8.44±0.12	8.59±0.51
			Fluvio-Lacustrine Sediments		
			Zelve Ign.	9.19±0.15	9.13±0.40
			Kavak4 Ign.		9.43±0.38
	Kavak3 Ign. Fluvio-Lacustrine Sediments	9.20±0.10 AFD: 9.08±0.06	AFD: 10.0±0.5		
	Kavak2 Ign. Fluvio-Lacustrine Sediments				
	Kavak1 Ign. Fluvio-Lacustrine Sediments	9.12±0.09	9.13±0.51		
	Damsa Lavas				
	Erdaş Andesite				
Upper Cretaceous	Basement		Acıgöl Granite	78.44±0.29	77.8±4.4

Fig. 3. Composite stratigraphic column and new crystallization and eruption ages for the CAVP. AFD = Air-fall deposit.

areas; Fig. 2) and in the vicinity of the Ecemiş fault (Figs. 1 and 2). In the Kurşunlu tepe region, Sarımadentepe ignimbrite overlies a palaeosol developed above Zelve ignimbrite. A basal fall out deposit with a maximum thickness of ~1.5 m in the Çardak region is welded and displays inverse grading (details of field relations in electronic Appendix 4). The overlying main flow deposit is in gradational contact with an

underlying ~2–3 cm thick horizon of dark-brown and lithic-rich ash. It is strongly welded and displays columnar jointing and up-section color variations from pale yellow to brownish-scarlet. Pumice of Sarımadentepe ignimbrite are eutaxitic, low-vesicularity with plagioclase, biotite, clinopyroxene, and oxide phenocrysts in pale to dark yellowish and brownish matrix.

Table 2
 $^{40}\text{Ar}/^{39}\text{Ar}$ radiometric ages for CAVP ignimbrites.

Sample	Unit	UTM easting	UTM northing	Material	Total fusion age (Ma)	2 σ error	Plateau age (Ma)	2 σ error	N	MSWD	Isocron age (Ma)	2 σ error	$^{40}\text{Ar}/^{36}\text{Ar}$ initial	2 σ error	J
KPD-08-009	Kavak	659645	4276775	Feldspar	9.11	0.12	9.12	0.09	11/11	0.29	9.13	0.15	285	42	0.001810
KPD-08-016	Kavak	659645	4276775	Feldspar	9.22	0.11	9.20	0.10	9/11	0.39	9.16	0.24	296	73	0.001795
KPD-08-018	Sarımadentepe	662381	4265700	Feldspar	8.37	0.09	8.44	0.12	10/11	1.98	8.54	0.20	138	114	0.001690
KPD-08-021	Gördeles	661557	4262949	Feldspar	6.34	0.07	6.34	0.07	10/11	0.65	6.24	0.18	332	75	0.001762
KPD-08-023	Cemilköy	658734	4261370	Feldspar	7.08	0.09	7.20	0.09	8/11	0.88	7.37	0.25	126	182	0.001734
KPD-08-025	Kızılkaya	661493	4260438	Feldspar	5.07	0.09	5.19	0.07	8/10	0.92	5.20	0.08	294	3	0.001749
KPD-08-031	Tahar	673454	4268634	Feldspar	6.11	0.28	6.14	0.22	10/11	0.21	6.10	0.23	299	8	0.001673
KPD-08-034	Zelve	658675	4280901	Feldspar	9.07	0.08	9.08	0.06	9/11	0.34	9.03	0.13	302	13	0.001780
KPD-08-035	Kavak	659439	4285471	Feldspar	9.18	0.17	9.19	0.15	11/11	0.25	9.13	0.17	294	15	0.001707
KPD-08-039	Sofular	672489	4286122	Feldspar	8.16	0.10	8.17	0.08	11/11	0.14	8.16	0.10	297	23	0.001656
KPD-08-050	Valibabatepe	728262	4282640	Feldspar	2.39	1.13	2.52	0.49	9/9	0.69	2.42	0.60	295	7	0.001719
K-015	Acıgöl granite	632344	4267719	Feldspar	78.37	0.29	78.44	0.29	10/13	0.28	78.37	0.44	299	18	0.001992

Ages calculated using biotite monitor FCT-3 (28.04 Ma) and the total decay constant $\lambda = 5.530\text{E}-10/\text{yr}$. N is the number of heating steps (defining plateau/total); MSWD is an F-statistic that compares the variance within step ages with the variance about the plateau age. J combines the neutron fluence with the monitor age. Bold: ages used in Table 1 and Fig. 3.

2.6. Sofular ignimbrite

Sofular ignimbrite comprises a ~1 m thick fine-grained pumiceous fallout deposit overlain by ~25 m of a single flow unit. The flow deposit is indurated, ash-supported lithic- and pumice-poor with maximum pumice size typically <4 cm. Phenocrysts in pumice comprise plagioclase, biotite, and oxides.

Because of very limited exposure in the vicinity of its type locality (Sofular village; Fig. 2), the stratigraphic placement of the Sofular ignimbrite has been most contentious in the CAVP. Originally proposed as a “lenticil” between Valibabatepe and İncesu members (Pasquarè, 1968), it was subsequently placed between the Gördeles and Kızılkaya ignimbrites (Le Pennec et al., 1994). Mues-Schumacher

and Schumacher (1996), however, suggested that the Sofular ignimbrite is the distal facies of the Valibabatepe ignimbrite, whereas Le Pennec et al. (2005) argued for Sofular being the distal facies of the Gördeles ignimbrite. More recently, Viereck-Götte et al. (2010) used geochemical and mineralogical data to correlate the “Sofular lenticil” with the “Sarımadentepe member” of Pasquarè (1968). Here, we propose that Sofular unit is a separate ignimbrite unit as constrained by radiometric dating and geochemical identity.

2.7. Cemilköy ignimbrite

This member represents an extensive and voluminous unit with an estimated volume of 300 km³, covering 8600 km² (Le Pennec et al., 1994). This ignimbrite was sufficiently voluminous to regionally fill in the paleomorphology, creating a volcanic peneplain. It characteristically forms smooth surfaces with prominent erosion features (“fairy chimneys”) due to its unwelded nature.

Only in Soğanlı valley, around Cemilköy, Yüksekli (North of Kızılrırmak valley), Keşlik villages and at Kolkolu Tepe (Southeast of Ayvalı) (Fig. 2), a thin, slightly altered pre-ignimbrite fallout deposit with lapilli-sized pumice is observed beneath the main ignimbrite flow. The main ignimbrite body is pale-gray, containing white-pale pumice in prismatic shapes with strongly flattened and elongate vesicles (“slaty fabric” in Le Pennec et al., 1994). Pumice in the flow occurs inversely graded with a maximum pumice size of 70 cm. The lithic clasts comprise volcanic clasts in Damsa valley, and ophiolitic rocks in Ayvalı region (Fig. 2), depending on locally exposed basement. Phenocrysts are plagioclase, biotite, amphibole, and oxides.

2.8. Local fallout deposits

In the Güzelöz, Tilköy, and Karain regions, fallout deposits, not evidently associated with any ignimbrites, are exposed (Fig. 2). Stratigraphically, these pumice layers have been variably placed between Kızılkaya and Cemilköy ignimbrites (Le Pennec et al., 1994; Toprak et al., 1994; Viereck-Götte et al., 2010). In the Güzelöz region, two pumiceous fallouts, separated by ~2 m of paleosol, are intercalated between Cemilköy and Gördeles ignimbrites. In vicinity of Tilköy, both fallout deposits are directly overlain by Kızılkaya ignimbrite. Viereck-Götte et al. (2010), based on the regional lithological, mineralogical, and geochemical similarities of pumice from different deposits, proposed that they are all stratigraphically equivalent. The eruption center may be located to the west of Tilköy/Derinkuyu (Viereck-Götte et al., 2010). We propose that they are correlative to the underlying Cemilköy ignimbrite (see below).

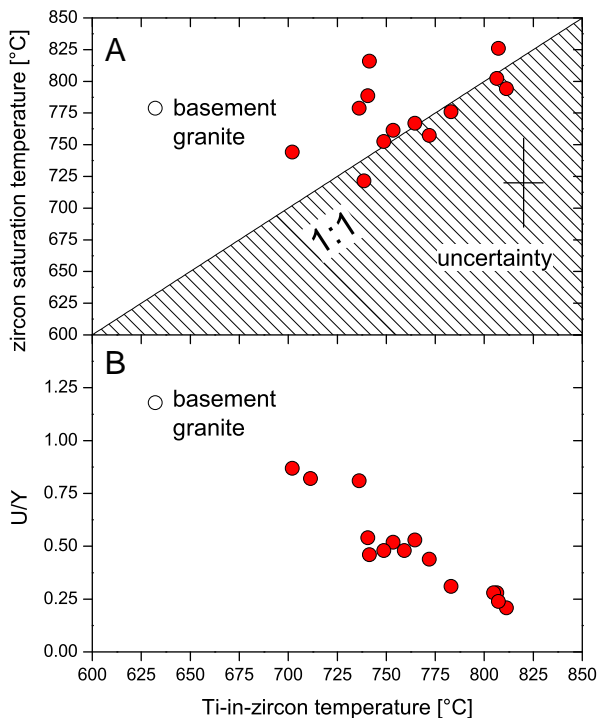


Fig. 4. Zircon saturation (a) and U/Y (b) vs. Ti-in-zircon temperature in CAVP ignimbrites (closed circles). Basement granite (sample K-015) values shown for comparison (open circle). Note that hatched region in lower right of the diagram is “forbidden” because this would imply zircon crystallization at super-saturation temperatures. All data (within uncertainty) are consistent with crystallization at temperature near or below the saturation temperature.

2.9. Tahar ignimbrite

This ignimbrite is restricted to the eastern part of the CAVP. It is distributed over 1000 km² with an estimated volume of 25 km³ (Le Pennec et al., 1994). It is generally pale-pink to scarlet-brown and mostly unwelded, but welding and columnar jointing is prominent around Sofular village. Its type locality is Tahar (Yeşilöz) village where it is ~120 m thick (Fig. 2; electronic Appendix 5). The thickness of the Tahar ignimbrite decreases in all directions from Hodul Dag, correlating with decreasing maximum lithic clast size. This implies a source location near Hodul Dag (Le Pennec et al., 1994). The sequence starts with alternating lapilli and ashy fallout deposits (~4 m thick near Yeşilöz) which are directly overlain by at least three successively emplaced flow deposits, separated by thin fallout deposits. Overall, Tahar ignimbrite is very rich in lithics, especially at the base of the flow. Glassy, beige to pinkish pumice with incipiently flattened vesicles is typical for the main flow deposit. It contains phenocrysts of plagioclase, amphibole, clinopyroxene, and orthopyroxene. At Yeşilöz, the Tahar ignimbrite is deposited on lacustrine sediments and overlain by lava flows.

2.10. Gördeles ignimbrite

This member has an estimated extent of ~3600 km² and a total volume of 110 km³ (Le Pennec et al., 1994). In the field, Gördeles can be confused with Kızılkaya or Sarımadentepe ignimbrites which all are incipiently to moderately welded and pale gray to light brownish in color. We distinguish two different units of Gördeles (Lower and Upper) which are separated by a paleosol (stratigraphic details in electronic Appendix 6). A lag breccia layer with gas escape pipes is present at the base of the Lower Gördeles around Kayırlı village (SW part of map in Fig. 2). Nearby, at Şahinkalesi tepe, the presence of lithic-rich lag breccias with pumices >60 cm indicates proximity to the vent (Le Pennec et al., 1994). The Upper Gördeles has a thin pumiceous fallout deposit directly overlain by ground surge deposits. These two basal layers are reliable field indicators for the Upper

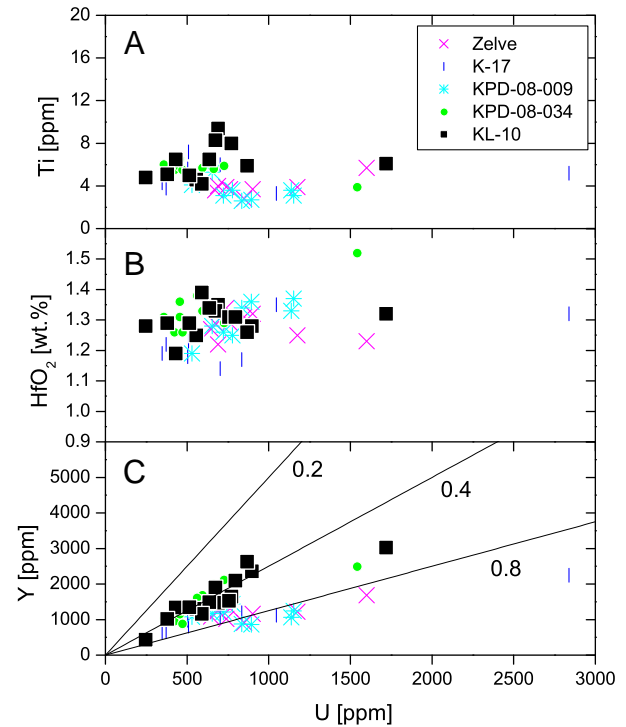


Fig. 6. Zircon trace element variation diagrams for Kavak and Zelve ignimbrites.

Gördeles, which mainly extends toward to east of the plateau. The main flow unit contains pumice with textural differences (fibrous vs. sub-spherically vesiculated) and color variations ranging from pale-brown to bright-white which are, however, compositionally identical. Phenocrysts are plagioclase, biotite, clinopyroxene, and oxides.

2.11. Kızılkaya ignimbrite

This is the most widespread ignimbrite unit in the CAVP where it forms flat surfaces over an area of ~8500–10600 km² with a volume of 180 km³ (Le Pennec et al., 1994; Schumacher and Mues-Schumacher, 1996). It is incipiently to strongly welded with occasional columnar jointing. Its average thickness varies between 13 and 15 m, classifying it as a low aspect ratio ignimbrite (Schumacher and Mues-Schumacher, 1996). Locally, thicknesses reaches >40–50 m (e.g., the Derinkuyu underground city) and peak at ~80 m (Ihlara valley).

Kızılkaya ignimbrite consists of a basal pre-ignimbrite Plinian fallout deposit and two main flow units separated by a flow discontinuity. Pumice glass in the lower flow unit is also more strongly vapor-phase altered compared to the upper flow. Texturally, Kızılkaya pumice resembles Gördeles ignimbrite pumice, with similar phenocrysts of plagioclase, biotite, orthopyroxene, and oxides.

2.12. Valibabatepe ignimbrite

This is another low-aspect ratio (5200 km², 100 km³; Le Pennec et al., 1994) ignimbrite in the CAVP. It is dark, strongly welded, and displays eutaxitic textures and well-developed fiamme. Outcrops are extensive in the eastern parts of the CAVP where it reaches a maximum thickness of 40 m around Talas, at the base of Mt. Erciyes from which it originated (Şen et al., 2003). Basal Plinian fallout deposits contain dacitic pumice with a modal mineral assemblage of plagioclase, amphibole, and clinopyroxene. The absence of biotite is one of the main field characteristics of the Valibabatepe ignimbrite. The designation Incesu

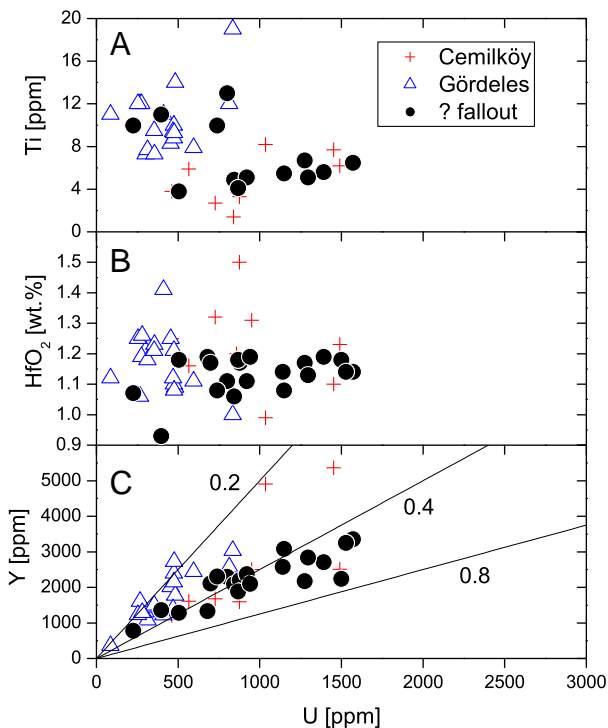


Fig. 5. Zircon trace element variation diagrams for Cemilköy and Gördeles ignimbrites in comparison to zircon from fallout deposits overlying Cemilköy ("?fallout").

is also used in the literature for this ignimbrite, but we prefer the original name Valibabatepe (Pasquare, 1968).

2.13. Kumtepe ignimbrite

The youngest ignimbrite in the CAVP erupted from the Quaternary Acıgöl Volcanic Complex located in its western part (Druitt et al., 1995; Schmitt et al., 2011). It was formed by two consecutive eruptions whose deposits are locally separated by paleosol and cinder cone deposits (Druitt et al., 1995). The Lower Acıgöl Tuff (= Lower Kumtepe) comprises lapilli-sized fallout interbedded with multiple ash layers and a single flow deposit. The Upper Acıgöl Tuff (Upper Kumtepe) has a basal lapilli fallout deposit which differs from the Lower Acıgöl Tuff by abundant obsidian lithic clasts. It is overlain by a pale pinkish to beige flow unit. Although geochemically nearly identical, marginal differences in crystal abundance exist: the lower tuff contains glassy, aphyric, and moderately vesicular pumice with very rare plagioclase and biotite microphenocrysts, whereas crystal content (plagioclase, biotite, oxides) is slightly higher in the upper tuff. The names Upper and Lower Acıgöl Tuffs were introduced because they originated from the Acıgöl caldera (Druitt et al., 1995; Fig. 2), with widely dispersed fallout deposits over Cappadocia and flow deposits to the north and east. To the south, flows onlap the pre-existing Erdaş Massif (Fig. 2). Henceforth, we subsume the Upper and Lower Acıgöl Tuffs under the term Kumtepe Ignimbrite (Pasquare, 1968).

2.14. Sampling strategy

During multiple field campaigns between 2008 and 2010, unaltered fresh rock samples were collected for mineralogical, geochemical, and geochronological analyses (sampling locations in Tables 2 and 3; electronic Appendix 1). Sampling targeted pumice from key ignimbrite units throughout the exposed sections including fallout and flow deposits, as well as epiclastic sedimentary deposits. Isopachs and isopleth maps for juvenile and accidental clast components were generated. Geophysical investigations included Anisotropy of Magnetic Susceptibility (AMS) analysis to constrain flow directions from ignimbrite drill cores. We obtained a total of 554 whole-rock geochemical analyses obtained by inductively coupled plasma (ICP) emission spectroscopy (ES) and mass spectrometry (MS) for major and trace elements,

respectively (ACME Labs). Thin-sections of all samples were prepared at Hacettepe University, Department of Geological Engineering, where mineral chemistry was analyzed on 45 selected samples using a Carl-Zeiss EVO-50 EP Scanning Electron Microscope (SEM) equipped with Bruker-Axis XFlash 3001 SDD-EDS. Publication of the entire geochemical data set is anticipated in a separate study. Here, we only draw on a few sub-aspects of these results as they pertain to our geochronological data (Tables 2 and 3).

3. Methods

3.1. U–Pb, trace element, and oxygen isotopes in zircon

Zircon was extracted from composite pumice samples following crushing and dissolution with cold 40% HF. Crystals were hand-picked from the HF indigestible residue, placed on adhesive tape, and cast in Buehler Epoxycure resin. Polishing was conducted with SiC coated-paper and 1 μm diamond suspension. Zircons were imaged using backscatter-electron and cathodoluminescence (CL) detectors on the University of California Los Angeles (UCLA) Leo VP1430 SEM.

After cleaning (1 N HCl, deionized water), a conductive Au layer was applied. Secondary ionization mass spectrometry (SIMS, ion microprobe) analyses were performed using a CAMECA ims 1270 at UCLA. The sequence and protocols we followed were to analyze oxygen isotopes first (Trail et al., 2007), followed by U–Pb and trace elements (Schmitt et al., 2003). This sequence avoids contamination of oxygen in zircon by ¹⁶O implanted under primary ion beam bombardment during U–Pb analysis. All U–Pb ages were corrected for common Pb using ²⁰⁷Pb and ²³⁰Th disequilibrium following procedures summarized in Schmitt et al. (2003).

One important analytical modification was that we also included trace elements at mass/charge stations 49 (⁴⁹Ti⁺), 57 (⁵⁷Fe⁺), 88.5 (¹⁷⁷Hf⁺⁺) 89 (⁸⁹Y⁺), and 196 (¹⁸⁰HfO⁺) in addition to the Zr, Pb, Th, and U species routinely analyzed. A 30 eV offset was applied to ¹⁷⁷Hf⁺⁺ and ⁸⁹Y⁺ to suppress potential molecular interferences, and the mass/charge = 89 peak was corrected for a minor interference of ¹⁷⁸Hf⁺⁺ using measured ¹⁷⁷Hf⁺⁺. Trace element concentrations were calculated using sensitivity factors relative to ⁹⁴Zr₂O⁺ from analysis of 91500 standard zircon using Zr-internal-standard values except for Hf for which an electron probe microanalysis working value was used (Table 2 in Liu et al., 2010). Analysis of ⁵⁷Fe⁺ aids

Table 3
U–Pb zircon ages, trace element compositions, and oxygen isotopic compositions of CAVP ignimbrites.

Sample	Unit	UTM easting	UTM northing	²⁰⁶ Pb/ ²³⁸ U age (Ma)	2σ error	N	MSWD	δ ¹⁸ O (‰)	2σ error	U/Y average	Ti average (ppm)	Ti min (ppm)	Ti max (ppm)	T(Ti) average (°C)	T(Ti) min (°C)	T(Ti) max (°C)	T(Sat) (°C)
K-287	? fallout	668597	4251465	6.90	0.34	10	1.45	5.70	0.27	0.44	6.6	3.3	11	772	−63	53	757
K-372	? fallout	669989	4261766	6.76	0.30	10	0.46	5.49	0.21	0.52	5.4	3.5	8.8	753	−39	48	762
KL-17	Kavak	659575	4276850	9.43	0.38	9	0.39	6.82	0.40	0.82	3.4	2.5	5.0	711	−28	33	–
KPD-08-004	? fallout	658460	4253373	6.96	0.28	10	0.59	5.41	0.40	0.54	4.7	3.4	5.7	741	−30	17	789
KPD-08-009	Kavak	659645	4276775	9.95	0.49	8	0.25	6.09	0.18	0.81	4.5	2.9	6.3	736	−39	31	779
KPD-08-034	Kavak	658675	4280901	10.0	0.5	8	0.52	7.06	0.17	0.87	3.1	2.2	4.6	702	−26	37	744
KL-01	Sarımadentepe	662886	4265561	8.59	0.51	10	0.47	5.04	0.33	0.21	9.6	6.7	16	811	−37	53	794
KL-02A	Gördeles rhyolite	661605	4263615	6.33	0.23	19	0.48	7.76	0.49	0.28	9.2	6.4	12	806	−37	29	802
KL-02B	Gördeles cumulate	"	"	"	"	"	"	6.66	0.77	0.28	9.1	6.4	17	805	−35	69	645
KL-03	Cemilköy	658718	4261333	6.66	0.40	10	1.51	5.87	1.21	0.48	4.6	2.4	7.2	739	−58	42	722
KL-05	Kızilkaya	668363	4261396	5.11	0.37	10	0.31	5.31	1.02	0.53	6.1	4.7	9.8	765	−25	48	767
KL-10	Kavak	659680	4276796	9.13	0.51	10	1.08	6.86	0.37	0.46	4.8	3.4	5.7	741	−30	16	816
KL-18	Zelve	659432	4285492	9.13	0.40	15	0.90	6.34	0.99	0.48	5.2	3.7	7.3	749	−31	33	753
KL-19	Sofular	672502	4286351	8.32	0.37	16	0.36	6.41	0.28	0.24	9.3	7.3	16	807	−24	61	826
KPD-08-031	Tahar	673454	4268634	6.07	0.67	1	–	4.54	0.52	0.31	6.3	–	–	768	–	–	776
K-015	Acıgöl Granite	632344	4267719	77.8	4.4	7	1.06	7.15	0.34	1.18	1.3	0.9	1.6	632	−23	16	779

All ages relative to AS3 zircon (1099.1 Ma) after correction for common Pb and initial disequilibrium. Bold: ages used in Table 1 and Fig. 3.

?Fallout: previously uncorrelated deposits overlying Cemilköy ignimbrite.

δ¹⁸O zircon in SMOW relative to AS3 zircon (5.34‰).

Ti averages, minima, and maxima values excluding high Fe/Zr analyses resulting from beam overlap onto crystal imperfections.

T(Ti) = Ti-in-zircon temperatures calculated for TiO₂ activity = 0.5 using calibration in Ferry and Watson (2007).

T(Sat) = zircon saturation temperatures from whole-rock pumice compositions using calibration in Watson and Harrison (1983).

in monitoring beam-overlap onto inclusions (e.g., glass, Fe–Ti oxides) in zircon, but because reliable Fe concentration data for 91500 are unavailable, we only report Fe/Zr relative to the maximum Fe/Zr in 91500 (electronic Appendix 7). Fe/Zr significantly elevated relative to 91500 (i.e., $>1 + 10\%$ estimated uncertainty), indicates potential beam overlap onto glass or Fe–Ti oxide inclusions in zircon, and we consequently discarded the corresponding Ti values. Replicate analysis of zircon AS3 (Duluth gabbro; [Paces and Miller, 1993](#)) yielded concentrations of Ti = 29.6 ± 5.9 ppm, Y = 2374 ± 874 ppm, and HfO₂ = 1.25 ± 0.24 wt.% relative to the 91500 standard.

3.2. ⁴⁰Ar/³⁹Ar geochronology

The samples analyzed by ⁴⁰Ar/³⁹Ar incremental heating experiments were plagioclase separates prepared from whole rock pieces from the pyroclastic units. Visibly obvious alteration was first removed using a rock saw. This was followed by crushing the samples using a porcelain jaw crusher, until approximately 25% of the grains were sieved into the 210–300 μm fraction. This size fraction was rinsed several times using ultra-pure de-ionized water and set in a 40 °C oven to dry overnight. The samples were further processed using a Frantz magnetic separator to concentrate the non-magnetic feldspar fraction from the remaining phases. All samples were cleaned by acid leaching in 1 N HCl (60 min), 6 N HCl (60 min), 1 N HNO₃ (60 min) and ultra-pure de-ionized water (60 min) in an ultrasonic bath heated to ~50 °C. Before irradiation approximately 100 mg of each plagioclase concentrate was hand-picked using a binocular microscope to remove any grains containing (remaining) alteration or other phases. Finally, these plagioclase separates were acid leached with 5% HF (15 min) to gently etch away the (altered) rims of the crystals.

Approximately 50 mg of plagioclase was irradiated for 6 h in the TRIGA CLICIT nuclear reactor at Oregon State University, along with the FCT-3 biotite (28.03 ± 0.18 Ma, 1σ) flux monitor ([Renne et al., 1998](#)). Individual J-values for each sample were calculated by parabolic extrapolation of the measured flux gradient against irradiation height and typically give 0.3–0.5% uncertainties (1σ). The ⁴⁰Ar/³⁹Ar incremental heating age determinations were performed using a continuous 10 W CO₂ laserprobe combined with a MAP-215/50 mass spectrometer at Oregon State University. Irradiated samples were loaded into Cu-planchettes in an ultra high vacuum sample chamber and incrementally heated by scanning a defocused CO₂ laser beam in preset patterns across the sample in order to evenly release the argon gas. After heating, reactive gases were cleaned up using an SAES Zr–Al ST101 GP50 getter operated at 400 °C for ~15 min and two SAES Fe–V–Zr ST172 getters operated at 200 °C and room temperature, respectively. Before analyzing a sample, and after every three heating steps, system blanks were measured. Data peak intensities were reduced using linear or exponential curve fits with respect to the inlet time of the gas sample into the mass spectrometer. All ages were calculated using the corrected ([Steiger and Jäger, 1977](#)) decay constant of $5.530 \pm 0.097 \times 10^{-10}$ 1/a (2σ) as reported by ([Min et al., 2000](#)). For a detailed description of the analytical facility and the constants used in the age calculations we refer to Table 2 in [Koppers et al. \(2003\)](#).

We calculated plateau ages and isochron ages as weighted means with $1/\sigma^2$ as weighting factor and as YORK2 least-square fits with correlated errors using the ArArCALC v2.5 software that is available from the <http://earthref.org/tools/ararcalc.htm> website ([Koppers, 2002](#), and references therein). Plateau ages and isochrons with values for the mean square of weighted deviates (MSWD) higher than unity were taken to indicate an increased scatter due to geological uncertainties beyond the precision of the increment ages themselves. In these cases the reported analytical errors are multiplied by the square-root of the MSWD. In this paper (see also summary in electronic Appendix 8), all errors on the ⁴⁰Ar/³⁹Ar ages are reported at the 95% confidence level (2σ).

4. Results

4.1. ⁴⁰Ar/³⁹Ar eruption ages

Plagioclase ⁴⁰Ar/³⁹Ar plateau and isochron ages were obtained from 8 to 11 heating steps, after excluding low temperature steps that yielded lower ages indicating minor ⁴⁰Ar loss. Because of the better analytical precision, we focus in this report on ⁴⁰Ar/³⁹Ar plateau ages, emphasizing that plateau and isochron ages are consistent (Table 2). Initial ⁴⁰Ar/³⁶Ar, determined from the isochron intercept, is generally indistinguishable from the air value, but comparatively imprecise intercepts result from clustering of the step isotopic compositions for Sarımadentepe (KPD-08-018) and Cemilköy (KPD-08-023) samples. In both these cases, however, we have no indication for significant excess ⁴⁰Ar. Ages decrease up-section, with overlapping ages of 9.11 ± 0.04 Ma (weighted mean of three analyses) and 9.08 ± 0.06 Ma (MSWD = 0.34) for Kavak and Zelve, respectively. Resolvably younger ages are obtained for Sarımadentepe (8.44 ± 0.12 Ma; MSWD = 1.98) and Sofular ignimbrites (8.17 ± 0.08 ; MSWD = 0.14). ⁴⁰Ar/³⁹Ar plagioclase ages for overlying Cemilköy (7.20 ± 0.09 Ma; MSWD = 0.88), Tahar (6.14 ± 0.22 Ma; MSWD = 0.21), and Gördeles ignimbrites (6.34 ± 0.07 Ma; MSWD = 0.65) are significantly older than the age of the capping and wide-spread Kızılkaya ignimbrite (5.19 ± 0.07 ; MSWD = 0.92), but age differences are irresolvable between Tahar and Gördeles. The youngest pre-Quaternary ignimbrite unit is the locally distributed Valibabatepe (2.52 ± 0.49 Ma; MSWD = 0.69). We consider the significance of these ages as eruption ages in the light of complementary ²⁰⁶Pb/²³⁸U zircon geochronology.

4.2. ²⁰⁶Pb/²³⁸U zircon crystallization ages

Typically, 10–15 spot analyses were conducted per sample, targeting U-rich domains in the zircon crystals using CL dark regions as a proxy (e.g., [Miller and Wooden, 2004](#)). Individual samples generally yielded uniform ²⁰⁶Pb/²³⁸U ages from which weighted average zircon crystallization ages are calculated (Table 3). The exceptions are sample KL-03 (Cemilköy) and KPD08-031 (Tahar) which yielded heterogeneous ²⁰⁶Pb/²³⁸U ages (discussed below), and only the youngest crystal (or coherent crystal population) was used for calculating crystallization ages. The late erupted and least silicic unit (Valibabatepe ignimbrite) lacks zircon. This is in contrast to [Viereck-Götte et al. \(2010\)](#) who described accessory zircon in Valibabatepe (Incesu in their terminology), whereas many other ignimbrites for which Table 4 in [Viereck-Götte et al. \(2010\)](#) does not list zircon have in fact yielded abundant zircon crystals (including Kızılkaya, Gördeles, Tahar, and Cemilköy).

CAVP ignimbrite zircon crystallization ages decrease upward with stratigraphical position and ⁴⁰Ar/³⁹Ar eruption age. ²⁰⁶Pb/²³⁸U zircon ages range between 9.63 ± 0.40 Ma (MSWD = 4.2; average of four samples) for Kavak and 5.11 ± 0.37 Ma (MSWD = 0.31) for Kızılkaya. Differences between crystallization and eruption ages are within analytical uncertainty for most samples, but for two Kavak ignimbrite samples (KPD-08-009 and KPD-08-034) pre-eruptive zircon residence over $\sim 0.9 \pm 0.4$ Ma can be resolved. In the case of Cemilköy ignimbrite (KL-03), the average ²⁰⁶Pb/²³⁸U zircon age is significantly younger than the ⁴⁰Ar/³⁹Ar age (-0.54 ± 0.37 Ma). KL-03 is also unusual in that a comparatively large fraction (~25%) of the analyzed zircon crystals yielded older ages: one out of 14 crystals analyzed is a Cretaceous xenocryst (106 ± 6 Ma), and three crystals yielded ages around $\sim 9 \pm 1$ Ma, similar in age to zircon from underlying Kavak and Zelve ignimbrites. The three antecrysts are unlikely to be magmatic because of the geographically separated eruption centers for Cemilköy and Kavak/Zelve ([Froger et al., 1998](#)). We therefore suspect that crystals became entrained during the eruption, and that plagioclase may also be in part xenocrystic, which could contribute excess ⁴⁰Ar if degassing was incomplete (e.g., [Spell et al., 2001](#)). We

therefore use the average zircon age of 6.66 ± 0.40 Ma (MSWD = 1.5) as a proxy for the Cemilköy eruption age. This eruption age estimate is consistent with $^{40}\text{Ar}/^{39}\text{Ar}$ and $^{206}\text{Pb}/^{238}\text{U}$ ages for the overlying ignimbrites (Gördeles and Tahar), which implies that zircon crystallization and eruption for Cemilköy occurred within a very brief interval (i.e., 0.3 ± 0.4 Ma). A second sample with heterogeneous zircon ages is Tahar (KPD08-031). Only one of the two processed Tahar composite pumice samples yielded few zircon crystals. One Tahar zircon crystal is Cretaceous (~ 75 Ma), and two crystals are Miocene (~ 7.8 Ma). This, however, pre-dates the eruption age of the underlying Cemilköy ignimbrite. Only one crystal yielded an age of 6.07 ± 0.67 Ma. This age is consistent with the $^{40}\text{Ar}/^{39}\text{Ar}$ age of the same sample (6.14 ± 0.22 Ma) which we adopt as the eruption age for Tahar.

4.3. Zircon chemistry

A significant volume of CAVP ignimbrites was deposited within brief periods lasting 1–2 Ma where eruption and crystallization ages frequently overlap within analytical uncertainties (Tables 1 and 2). This limits geochronology as a correlation tool. Zircon geochronology has been applied previously to correlate proximal and distal ashes of the Bishop Tuff (Schmitt and Hulen, 2008), but zircon compositions thus far have not been rigorously tested for distinguishing ignimbrite units within an individual province. The advantage of zircon lies in its resistance to alteration, and it can display compositional variability that to a first order is controlled by magmatic temperature, degree of fractionation, and magma source compositions. The saturation of zircon is well constrained as a function of melt composition and temperature (Watson and Harrison, 1983), Ti-in-zircon is calibrated as a magmatic thermometer (Ferry and Watson, 2007), Y, Hf, and U typically increase with differentiation (Claiborne et al., 2006), and higher $\delta^{18}\text{O}$ zircon reflects contribution of continental crustal sources relative to mantle (Trail et al., 2007). The validity of these assumptions is supported in our data by a broad correlation between U/Y and Ti-in-zircon temperatures (reflecting higher degrees of differentiation with decreasing temperature; Fig. 4). Ti-in-zircon temperatures (for titania activity $a_{\text{TiO}_2} = 0.5$; Ferry and Watson, 2007) and zircon saturation thermometry (using the calibration of Watson and Harrison, 1983) are consistent within calibration uncertainties of the thermometers, under the reasonable assumption that Ti-in-zircon temperatures must always be equal or less than the zircon saturation temperature (Fig. 4). Although systematic investigation of basement zircon was beyond the scope of our study, reconnaissance xenocryst analysis indicates that $\delta^{18}\text{O}$ in these zircons ($\delta^{18}\text{O} = 6.6$ and 10.2% for Cretaceous xenocrysts in Tahar and Cemilköy, respectively) exceeds mantle compositions ($\sim 5.3\%$; Trail et al., 2007). Elevated $\delta^{18}\text{O}$ values in CAVP zircon reflect extensive crustal assimilation, as indicated by overlapping $\delta^{18}\text{O}$ zircon values between some CAVP ignimbrites and local basement (i.e., Cretaceous Acıgöl granite with $\delta^{18}\text{O}$ zircon = $7.2 \pm 0.3\%$; Table 3).

Here, we explore the use of zircon geochemistry to resolve three specific problems related to CAVP ignimbrite correlation. First, we investigate zircon in three samples of fallout deposits stratigraphically placed between Cemilköy and Kızılkaya as “unknowns”. These samples (K-287, K-372, KPD-08-004), which were not dated by $^{40}\text{Ar}/^{39}\text{Ar}$ because of weathering, have similar average $^{206}\text{Pb}/^{238}\text{U}$ zircon ages. These ages overlap within uncertainty with the average zircon age of the underlying Cemilköy ignimbrite (KL-03). Gördeles and Tahar zircon ages are on average younger, but populations overlap. We can rule out correlation with Tahar because it is characterized by a scarcity of zircon which contrasts with abundant zircon in K-287, K-372, and KPD-08-004. Correlation with Gördeles can be dismissed because Gördeles zircons on average have higher Ti, and lower U and Y compared to the “unknowns”, although the ranges overlap (Fig. 5). HfO₂ is similar in all units (Fig. 5). Zircon oxygen isotopes in K-287, K-372, and KPD-08-004 cluster tightly ($\delta^{18}\text{O} = 5.7 \pm$

0.3% , $5.5 \pm 0.2\%$, and $5.4 \pm 0.4\%$, respectively), and are indistinguishable from the Cemilköy zircon average (KL-03 $\delta^{18}\text{O} = 5.9 \pm 1.2\%$). These values are significantly lower than those of Gördeles zircon for which two compositionally different pumice types (KL-02A and KL-02B) yielded higher values of $\delta^{18}\text{O} = 7.8 \pm 0.8\%$ and $6.7 \pm 1.1\%$, respectively. Cemilköy therefore appears to be the best match for the “unknown” fallout deposits.

Secondly, we tested for differences in zircon geochemistry between Kavak and superimposed Zelve ignimbrites, which have closely overlapping $^{40}\text{Ar}/^{39}\text{Ar}$ and $^{206}\text{Pb}/^{238}\text{U}$ zircon ages. Except for a broad correlation between Y and U, systematic variations between U and Ti or U and HfO₂ are absent (Fig. 6). There is a slight difference in the U/Y trends for Zelve and Kavak sample KL-10 on one hand (average U/Y ~ 0.4), and the remaining Kavak samples on the other (average U/Y ~ 0.8). Zelve and Kavak sample KL-10 also have overlapping average $^{206}\text{Pb}/^{238}\text{U}$ zircon ages, slightly younger than for other Kavak samples. Zircon oxygen isotopic compositions display an $\sim 1\%$ difference between Kavak samples (with average $\delta^{18}\text{O}$ ranging between $6.1 \pm 0.2\%$ and $7.1 \pm 0.2\%$), but lack a systematic trend with age. Collectively, geochronological and compositional data thus reveal close similarities between Zelve and Kavak ignimbrites, and they may in fact be erupted from the same source.

Lastly, correlations between Sofular and Gördeles ignimbrites (Le Pennec et al., 2005) and Sofular and Sarımadentepe (Viereck-Götte et al., 2010) have been proposed, which can be scrutinized using our zircon data. $^{40}\text{Ar}/^{39}\text{Ar}$ and $^{206}\text{Pb}/^{238}\text{U}$ dating indicates that Sofular is ~ 1.8 Ma older than Gördeles, consistent with stratigraphic relations described in Viereck-Götte et al. (2010). Dismissal of the proposed correlation between Sofular and Sarımadentepe ignimbrites is less straightforward because $^{206}\text{Pb}/^{238}\text{U}$ zircon ages overlap, although $^{40}\text{Ar}/^{39}\text{Ar}$ plateau ages are distinctively younger for Sofular (by 0.27 ± 0.14 Ma). Zircon trace element abundances (especially for Ti and Hf) are also very similar in Sofular and Sarımadentepe (as well as Gördeles) ignimbrites, with Gördeles having slightly higher U/Y than the other two units (Fig. 7). Differences exist in whole-rock trace element compositions, but compositions overlap (Fig. 8). Zircon oxygen

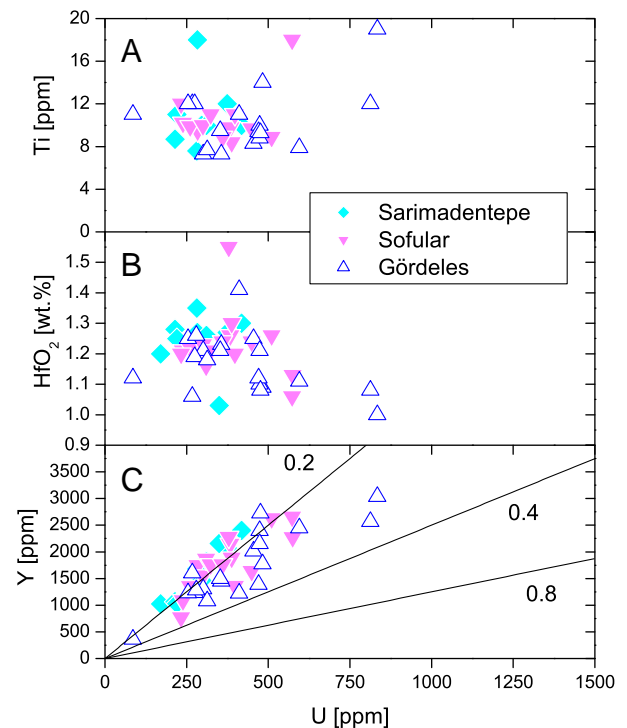


Fig. 7. Zircon trace element variation diagrams for Sofular, Sarımadentepe, and Gördeles ignimbrites.

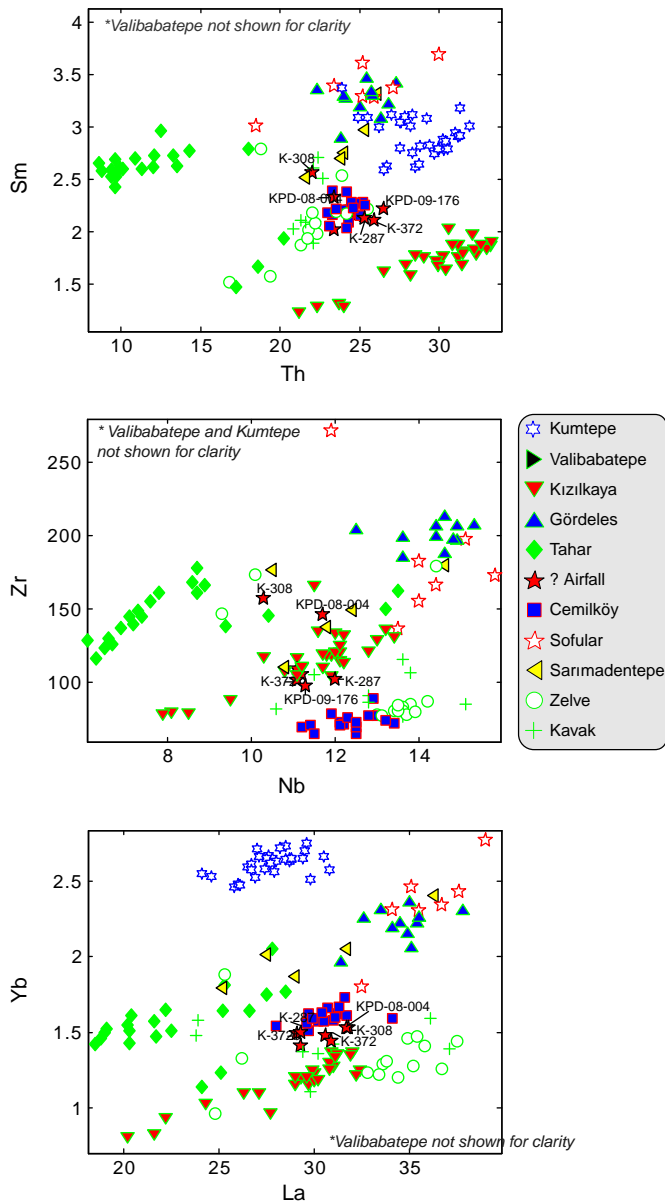


Fig. 8. Whole rock chemical correlations of CAVP ignimbrites.

isotopes, however, are significantly lower in Sofular ($\delta^{18}\text{O} = 6.1 \pm 0.2\text{‰}$) compared to Sarımadentepe ($\delta^{18}\text{O} = 5.0 \pm 0.3\text{‰}$). This supports the minor, but significant difference in $^{40}\text{Ar}/^{39}\text{Ar}$ ages, and indicates that Sofular and Sarımadentepe in fact represent separate eruptions.

5. Discussion

5.1. A revised stratigraphic framework for the CAVP ignimbrites

Since the pioneering work of Pasquarè (1968) who classified volcanic and continental sedimentary units and introduced a naming scheme, the CAVP volcanostratigraphy has remained a matter of debate. We discuss new insights from geochronological and geochemical correlation from our data in stratigraphic order.

For the oldest ignimbrite, Kavak, we concur with previous researchers (Le Pennec et al., 1994, 2005; Mues-Schumacher and Schumacher, 1996; Viereck-Götte et al., 2010) on the existence of multiple units intercalated with epiclastic sediments. Because of tightly overlapping eruption and crystallization ages, as well as coherent zircon geochemical trends, we

maintain that grouping all Kavak ignimbrites (1–4) into a single Kavak member is justified. We acknowledge that equally close age and compositional relationships exist between Kavak and Zelve ignimbrites (Fig. 6), but because of its volume (1.5 times that of Kavak) and distinctive field characteristics, the Zelve ignimbrite is justifiably classified as a separate member.

$^{40}\text{Ar}/^{39}\text{Ar}$ feldspar and $^{206}\text{Pb}/^{238}\text{U}$ zircon ages for Sarımadentepe ignimbrite are consistent with published data, confirming the original volcanostratigraphy of Pasquarè (1968). $^{40}\text{Ar}/^{39}\text{Ar}$ feldspar and $^{206}\text{Pb}/^{238}\text{U}$ zircon ages for the basal plinian fallout of Sofular ignimbrite are the first of their kind, and although ages and some geochemical parameters (whole-rock major element compositions, zircon trace elements) are similar to those of Sarımadentepe ignimbrite, zircon $\delta^{18}\text{O}$ values and whole rock trace element compositions (Figs. 7 and 8) reveal differences between both units. Our data is also at variance with the proposal that Sofular ignimbrite is correlated to Gördeles ignimbrite (Le Pennec et al., 2005). This suggestion was based on observations in an outcrop near Topuzdağ (Fig. 2), where Tahar ignimbrite apparently overlies Sofular ignimbrite. At this locale, however, Tahar ignimbrite represents valley pond, whereas Sofular is present in a topographically higher position. Moreover, faulting that displaces Topuzdağ lavas, Sofular ignimbrite, and lacustrine deposits does not cut the Tahar ignimbrite. These structural relations are consistent with our radiometric dating results that demonstrate a ~ 1.8 Ma age gap between Tahar and Sofular ignimbrites. Hence, we maintain that the Sofular ignimbrite represents a distinct ignimbrite that is uncorrelated with any other CAVP member (cf., Le Pennec et al., 2005; Viereck-Götte et al., 2010).

The average $^{206}\text{Pb}/^{238}\text{U}$ zircon age obtained from Cemilköy ignimbrite (6.66 ± 0.40 Ma) is consistent with its stratigraphic position, and slightly older $^{40}\text{Ar}/^{39}\text{Ar}$ feldspar ages likely result from minor xenocrystic contamination. Local pumice fallout deposits overlying Cemilköy ignimbrites east of Derinkuyu that were termed “Güzeldere Member” by Viereck-Götte et al. (2010) have $^{206}\text{Pb}/^{238}\text{U}$ zircon ages, zircon trace elements, and zircon $\delta^{18}\text{O}$ that are close to those of Cemilköy ignimbrite. These pumice layers are well exposed in the vicinity of Tilköy below the Kızilkaya ignimbrite. In the Yeşilöz–Karain sector below the Tahar ignimbrite they occur interbedded within epiclastic sediments, and in the Güzeldere region two fallout layers separated by paleosol are intercalated between Cemilköy and overlying Gördeles ignimbrites. Our correlation with Cemilköy is supported by alteration-resistant whole-rock rare earth element (REE) data (Fig. 8). La abundance and La/Sm of Cemilköy ignimbrites are between 28 and 32 ppm and 13–14.5, respectively, which differ from most CAVP pumice except Kavak (La: 23–39 ppm; La/Sm: 11.5–15.5). La abundance (29–31 ppm) and La/Sm (13.5–14.5) of Güzeldere, Karain, and Tilköy fallout pumice match closely with those of Cemilköy, whereas correlation with Kavak can be dismissed because of its much older age (Fig. 8). We conclude that local fallout deposits share the same magmatic source with the Cemilköy ignimbrite, and we therefore subsume them under the Cemilköy ignimbrite member.

Our $^{40}\text{Ar}/^{39}\text{Ar}$ and $^{206}\text{Pb}/^{238}\text{U}$ chronostratigraphy confirms the stratigraphic positions of Tahar and Gördeles ignimbrites. Moreover, our ages for Kızilkaya ignimbrite reasonably agree with published K–Ar data of Innocenti et al. (1975) and Besang et al. (1977), but they are older than K–Ar ages in Mues-Schumacher and Schumacher (1996). $^{40}\text{Ar}/^{39}\text{Ar}$ plagioclase ages for Valibabatepe ignimbrite (2.52 ± 0.49 Ma) agree with K–Ar data in Innocenti et al. (1975). For the Kumtepe member, we refer to Schmitt et al. (2011) who presented a detailed geochronology of the Quaternary Acıgöl Volcanic Complex.

5.2. Pre-eruptive magmatic processes: crystal residence, recycling, and resorption

With a firm chronostratigraphy established, we can re-evaluate the magmatic evolution of the CAVP. Here, and in other ignimbrite

provinces, the differences between eruption and crystallization ages can provide a first-order estimate on magma volumes because zircon saturates upon cooling, and magmatic cooling rates scale with magma volume (e.g., Simon et al., 2008; Schmitt et al., 2011). These simple relations, however, can be obscured by processes such as crystal recycling from precursor plutonic rocks or older eruptions, yielding estimates for magma residence that are too high. Resorption of pre-existing crystals, by contrast, will underestimate residence timescales. In addition, analytical artifacts need to be considered for accurately constraining pre-eruptive crystallization duration. Whereas calibration uncertainties of decay constants (e.g., Min et al., 2000) are of second-order relevance given potentially large differences in $^{40}\text{Ar}/^{39}\text{Ar}$ eruption and $^{206}\text{Pb}/^{238}\text{U}$ crystallization ages (on average 80 ka; Simon et al., 2008), the impact of excess ^{40}Ar or crystal contamination in bulk analysis data can be severe, masking potential differences between eruption and crystallization ages.

In the case of the CAVP ignimbrites, extended zircon residence times ($\sim 0.9 \pm 0.4$ Ma) are detected for some Kavak ignimbrite units. The overlying Zelve ignimbrite, by contrast, displays negligible pre-eruptive zircon residence. Lack of resolvable zircon residence also characterizes the younger ignimbrites, including two of most voluminous CAVP ignimbrites (the $\sim 300 \text{ km}^3$ Cemilköy and $\sim 180 \text{ km}^3$ Kızılkaya ignimbrites; Le Pennec et al., 1994). Analytical uncertainties, however, are only permissible for estimating zircon residence within few ~ 100 s ka. Zircon residence over such time intervals is broadly consistent with other voluminous silicic eruptions, but the durations determined for the Miocene members of the CAVP are comparatively imprecise relative to Late Pleistocene ignimbrites in which high-precision U–Th zircon dating can be applied (e.g., Schmitt et al., 2011).

The observation that only few CAVP ignimbrites contain crystals that are older than their stratigraphic precursor contrasts with other long-lived continental silicic magma systems where crystal inheritance between subsequent eruptive episodes is more common (e.g., Heise Caldera; Bindeman et al., 2007, Southwestern Nevada Volcanic field; Bindeman et al., 2006; Cerro Galan; Folkes et al., 2011; Sierra Madre Occidental; Bryan et al., 2008). The absence of such crystals cannot be completely ruled out because we could only analyze a limited number of zircon crystals per sample in order to meet our goal of establishing a stratigraphic framework for the entire CAVP ignimbrite sequence.

Pre-Miocene xenocrysts are also scarce and were only encountered in Tahar and Cemilköy ignimbrites. Again, our reconnaissance sampling does not warrant a strong interpretation of these findings, but the scarcity of crustal xenocrysts seems at variance with significant crustal assimilation indicated by elevated $\delta^{18}\text{O}$ in zircon for some of the ignimbrites. This apparent conflict can be resolved if crustally derived zircons became resorbed in a hot (and wet) magma prior to eruption.

We therefore hypothesize that protracted zircon crystallization (and preservation of crustally derived xenocrysts) is a hallmark of the waxing stages of ignimbrite volcanism during which multiple small-volume intrusions cooled rapidly, resulting in collectively protracted zircon crystallization. When individual intrusions coalesced into an eruptible magma chamber, they produced a wide spectrum of zircon ages via crystal recycling. With time, continued mafic intrusion further heated the crust so that after an initial lag period (e.g., Annen, 2009) the shallow crustal magma storage region reached elevated temperatures, and potentially became more mafic. Such conditions would be conducive to rapid resorption of any pre-existing zircon xeno- or antecrysts (Harrison and Watson, 1983). The resulting zircon populations display a unimodal age distribution because they crystallized during cooling shortly before eruption. This model is supported by evidence for thermal cycling recorded in Ti-in-zircon temperatures for the CAVP (Fig. 9): within the two main eruptive pulses at ~ 9.1 – 8.4 Ma (Kavak, Zelve, and Sarımadentepe) and

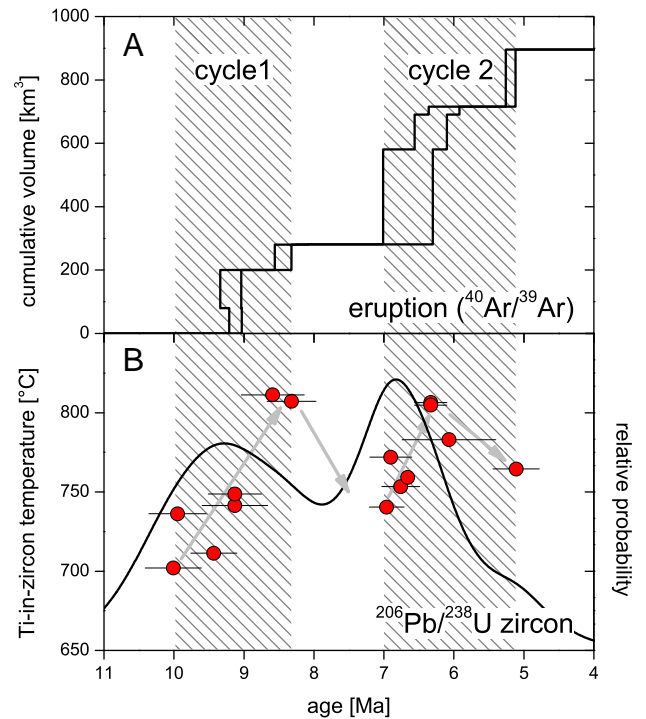


Fig. 9. Cumulative erupted volumes (after Le Pennec et al., 1994) vs. eruption age (a) and Ti-in-zircon temperature vs. $^{206}\text{Pb}/^{238}\text{U}$ zircon crystallization ages (as sample averages, and probability density plot) (b). Episodes of peak activity (phases 1 and 2) correspond to elevated magmatic temperatures recorded in zircon (see text).

~ 6.7 – 5.1 Ma (Cemilköy, Gördeles, and Kızılkaya) higher zircon crystallization temperatures characterize the peak-eruption units compared to their precursors. These observations suggest repeated episodes of thermal maturation, where high extrusion rates that are typical for continental ignimbrite flare-ups ($10^{-3} \text{ km}^3/\text{year}$; de Silva and Gosnold, 2007) are reached when the crust is at its thermal peak, whereas the time-integrated productivity of the CAVP remained lower by a factor of ~ 10 (Fig. 9).

6. Conclusions

$^{40}\text{Ar}/^{39}\text{Ar}$ and U–Pb chronology has refined the chronostratigraphic framework for the CAVP, one of the world's best exposed and preserved ignimbrite provinces. Ages and chemical characteristics of whole-rock pumice and zircon reveal strong similarities between sequential eruptions that collectively comprise the Kavak and Cemilköy ignimbrite members (sensu Pasquarè, 1968). This argues against subdividing within these members (cf. Viereck-Götte et al., 2010). In other instances, we have demonstrated significant chemical and age differences between previously correlated units: $\delta^{18}\text{O}$ in zircon differs by $\sim 1\%$ between Sofular and Sarımadentepe ignimbrites, and Sofular is ~ 1.8 Ma older than Gördeles ignimbrites. This is at variance with correlations proposed by Viereck-Götte et al. (2010) and Le Pennec et al. (2005), respectively.

The new ages permit detailed reconstruction of eruptive volumes and pre-eruptive magma storage conditions (through zircon thermometry and residence times based on the difference between $^{40}\text{Ar}/^{39}\text{Ar}$ eruption and U–Pb zircon crystallization ages). The CAVP eruptions have occurred in two main pulses (~ 9 – 8 Ma and ~ 7 – 5 Ma) separated by an ~ 1 Ma hiatus. Each pulse shows an ~ 75 – 100 °C increase in zircon crystallization temperature and a decreasing abundance of pre-existing zircon. This implies that accumulation of eruptible evolved magma at shallow crustal levels occurred during short-lived (1–2 Ma) episodes of high magma flux rates. During these episodes, erupted volumetric

rates peak at values that are commensurate to those in other continental ignimbrite provinces ($\sim 10^{-3} \text{ km}^3/\text{a}$; De Silva and Gosnold, 2007).

Supplementary materials related to this article can be found online at doi:10.1016/j.jvolgeores.2011.11.005.

Acknowledgements

Journal reviewers Cathy Busby and Luca Ferrari provided constructive and helpful reviews. Janet C. Harvey is thanked for comments on an earlier manuscript. Different parts of this work were financially supported by Tubitak projects (108Y063 and Vertical Anatolian Movement Project-107Y333) and Hacettepe University BAB Project (0701602009). The ion microprobe facility at UCLA is partly supported by a grant from the Instrumentation and Facilities Program, Division of Earth Sciences, National Science Foundation.

References

- Annen, C., 2009. From plutons to magma chambers: thermal constraints on the accumulation of eruptible silicic magma in the upper crust. *Earth and Planetary Science Letters* 284 (3–4), 409–416.
- Aydar, E., Gourgaud, A., 1998. The geology of Mount Hasan stratovolcano, central Anatolia, Turkey. *Journal of Volcanology and Geothermal Research* 85 (1–4), 129–152.
- Aydar, E., Gourgaud, A., Deniel, C., Lyberis, N., Gundogdu, N., 1995. Le volcanisme quaternaire d'Anatolie centrale (Turquie): association de magmatisme calco-alcalin et alcalin en domaine de convergence. *Canadian Journal of Earth Sciences* 32 (7), 1058–1069.
- Besang, C., Eckhardt, F.J., Harre, W., Kreuzer, G., Müller, P., 1977. Radiometrische Altersbestimmungen an neogenen Eruptivgesteinen der Türkei. *Geologisches Jahrbuch* 25, 3–36.
- Beekman, P.H., 1966. The Pliocene and Quaternary volcanism in the HasanDag-Melenidiz Dag region. *Bulletin of MTA* 66, 90–105.
- Bindeman, I.N., Schmitt, A.K., Valley, J.W., 2006. U–Pb zircon geochronology of silicic tuffs from the Timber Mountain/Oasis Valley caldera complex, Nevada: rapid generation of large volume magmas by shallow-level remelting. *Contributions to Mineralogy and Petrology* 152 (6), 649–665.
- Bindeman, I.N., Watts, K.E., Schmitt, A.K., Morgan, L.A., Shanks, P.W.C., 2007. Voluminous low $\delta^{18}\text{O}$ magmas in the late Miocene Heise volcanic field, Idaho: implications for the fate of Yellowstone hotspot calderas. *Geology* 35 (11), 1019–1022.
- Bryan, S.E., Ernst, R.E., 2008. Revised definition of Large Igneous Provinces (LIPs). *Earth-Science Reviews* 86 (1–4), 175–202.
- Bryan, S.E., Ferrari, L., Reiners, P.W., Allen, C.M., Petrone, C.M., Ramos-Rosique, A., Campbell, I.H., 2008. New insights into crustal contributions to large-volume rhyolite generation in the Mid-Tertiary Sierra Madre Occidental Province, Mexico, revealed by U–Pb geochronology. *Journal of Petrology* 49 (1), 47–77.
- Cerling, T.E., Brown, F.H., Bowman, J.R., 1985. Low-temperature alteration of volcanic glass – hydration, Na, K, ^{18}O and Ar mobility. *Chemical Geology* 52 (3–4), 281–293.
- Claiborne, L.L., Miller, C.F., Walker, B.A., Wooden, J.L., Mazdab, F.K., Bea, F., 2006. Tracking magmatic processes through Zr/Hf ratios in rocks and Hf and Ti zoning in zircons: an example from the Spirit Mountain batholith, Nevada. *Mineralogical Magazine* 70 (5), 517–543.
- De Silva, S.L., 1989. Altiplano–Puna volcanic complex of the central Andes. *Geology* 17 (12), 1102–1106.
- De Silva, S.L., Gosnold, W.D., 2007. Episodic construction of batholiths: insights from the spatiotemporal development of an ignimbrite flare-up. *Journal of Volcanology and Geothermal Research* 167 (1–4), 320–335.
- Dilek, Y., Sandvol, E.A., 2009. Seismic structure, crustal architecture and tectonic evolution of the Anatolian–African Plate boundary and the Cenozoic orogenic belts in the eastern Mediterranean region. *Geological Society of America Special Publication* 327, 127–160.
- Druitt, T.H., Brencley, P.J., Gökten, Y.E., Francaviglia, V., 1995. Late-Quaternary rhyolitic eruptions from the Acıgöl Complex, central Turkey. *Journal of the Geological Society (London, United Kingdom)* 152, 655–667.
- Ferrari, L., Lopez-Martinez, M., Rosas-Elguera, J., 2002. Ignimbrite flare-up and deformation in the southern Sierra Madre Occidental, western Mexico: implications for the late subduction history of the Farallon plate. *Tectonics* 21 (4). doi:10.1029/2001TC001302.
- Ferry, J.M., Watson, E.B., 2007. New thermodynamic models and revised calibrations for the Ti-in-zircon and Zr-in-rutile thermometers. *Contributions to Mineralogy and Petrology* 154 (4), 429–437.
- Folkes, C.B., De Silva, S.L., Schmitt, A.K., Cas, R.A.F., 2011. A reconnaissance of U–Pb zircon ages in the Cerro Galán system, NW Argentina: prolonged magma residence, crystal recycling and crustal assimilation. *Journal of Volcanology and Geothermal Research* 206 (3–4), 136–147.
- Froger, J.-L., Lénat, J.-F., Chorowicz, J., Le Pennec, J.-L., Bourdier, J.-L., Köse, O., Zimitoglu, O., Gündogdu, N.M., Gourgaud, A., 1998. Hidden calderas evidenced by multisource geophysical data; example of Cappadocian Calderas, Central Anatolia. *Journal of Volcanology and Geothermal Research* 185, 99–128.
- Glazner, A.F., Nielson, J.E., Howard, K.A., Miller, D.M., 1986. Correlation of the Peach Springs Tuff, a Large-Volume Miocene Ignimbrite Sheet in California and Arizona. *Geology* 14 (10), 840–843.
- Harrison, T.M., Watson, E.B., 1983. Kinetics of zircon dissolution and zirconium diffusion in granitic melts of variable water-content. *Contributions to Mineralogy and Petrology* 84 (1), 66–72.
- Hildreth, W., Mahood, G., 1985. Correlation of ash-flow tuffs. *Geological Society of America Bulletin* 96 (7), 968–974.
- Hora, J.M., Singer, B.S., Jicha, B.R., Beard, B.L., Johnson, C.M., de Silva, S., Salisbury, M., 2010. Volcanic biotite-sanidine $^{40}\text{Ar}/^{39}\text{Ar}$ age discordances reflect Ar partitioning and pre-eruption closure in biotite. *Geology* 38 (10), 923–926.
- Innocenti, F., Mazzuoli, R., Pasquarè, G., Radicati di Brozolo, F., Villari, L., 1975. The Neogene calc-alkaline volcanism of Central Anatolia: geochronological data on Kayseri–Nigde area. *Geological Magazine* 112, 349–360.
- Koppers, A.A.P., 2002. ArArCALC – software for $^{40}\text{Ar}/^{39}\text{Ar}$ age calculations. *Computers & Geosciences* 28 (5), 605–619.
- Koppers, A.A.P., Staudigel, H., Duncan, R.A., 2003. High-resolution $^{40}\text{Ar}/^{39}\text{Ar}$ dating of the oldest oceanic basement basalts in the western Pacific basin. *Geochemistry, Geophysics, Geosystems* 4. doi:10.1029/2003GC000574.
- Le Pennec, J.-L., Bourdier, J.-L., Froger, J.-L., Temel, A., Camus, G., Gourgaud, A., 1994. Neogene ignimbrites of the Nevşehir Plateau (Central Turkey), stratigraphy, distribution and source constraints. *Journal of Volcanology and Geothermal Research* 63, 59–87.
- Le Pennec, J.-L., Temel, A., Froger, J.-L., Sen, S., Gourgaud, A., Bourdier, J.-L., 2005. Stratigraphy and age of the Cappadocia ignimbrites, Turkey: reconciling field constraints with paleontologic, radiochronologic, geochemical and paleomagnetic data. *Journal of Volcanology and Geothermal Research* 141, 45–64.
- Liu, Y.S., Hu, Z.C., Zong, K.Q., Gao, C.C., Gao, S., Xu, J.A., Chen, H.H., 2010. Reappraisal and refinement of zircon U–Pb isotope and trace element analyses by LA-ICP-MS. *Chinese Science Bulletin* 55 (15), 1535–1546.
- McCulloch, M.T., Kyser, T.K., Woodhead, J.D., Kinsley, L., 1994. Pb–Sr–Nd–O isotopic constraints on the origin of rhyolites from the Taupo Volcanic Zone of New Zealand – evidence for assimilation followed by fractionation from basalt. *Contributions to Mineralogy and Petrology* 115 (3), 303–312.
- McDowell, F.W., 2007. Geologic transect across the northern Sierra Madre Occidental volcanic field, Chihuahua and Sonora, Mexico. *Geological Society of America Digital Map and Chart Series* 6, 1–70.
- Miller, J.S., Wooden, J.L., 2004. Residence, resorption and recycling of zircons in Devils Kitchen rhyolite, Coso Volcanic field, California. *Journal of Petrology* 45 (11), 2155–2170.
- Min, K.W., Mundil, R., Renne, P.R., Ludwig, K.R., 2000. A test for systematic errors in $^{40}\text{Ar}/^{39}\text{Ar}$ geochronology through comparison with U/Pb analysis of a 1.1-Ga rhyolite. *Geochimica Et Cosmochimica Acta* 64 (1), 73–98.
- Mues-Schumacher, U., Schumacher, R., 1996. Problems of stratigraphic correlation and new K–Ar data for ignimbrites from Cappadocia, central Turkey. *International Geology Review* 38 (8), 737–746.
- Notsu, K., Fujitani, T., Ui, T., Matsuda, J., Ercan, T., 1995. Geochemical features of collision-related volcanic rocks in central and eastern Anatolia, Turkey. *Journal of Volcanology and Geothermal Research* 64, 171–192.
- Paces, J.B., Miller, J.D., 1993. Precise U–Pb ages of Duluth complex and related mafic intrusions, northeastern Minnesota – geochronological insights to physical, petrogenetic, paleomagnetic, and tectonomagmatic processes associated with the 1.1 Ga midcontinent rift system. *Journal of Geophysical Research-Solid Earth* 98 (B8), 13997–14013.
- Pasquarè, G., 1968. Geology of the Cenozoic volcanic area of central Anatolia. *Atti Accademia Nazionale dei Lincei* 9, 55–204.
- Pasquarè, G., Poli, S., Vezzoli, L., Zanchi, A., 1988. Continental arc volcanism and tectonic setting in Central Anatolia, Turkey. *Tectonophysics* 146, 217–230.
- Perry, F.V., Depaolo, D.J., Baldrige, W.S., 1993. Neodymium isotopic evidence for decreasing crustal contributions to Cenozoic ignimbrites of the western United States – implications for the thermal evolution of the Cordilleran crust. *Geological Society of America Bulletin* 105 (7), 872–882.
- Renne, P.R., Swisher, C.C., Deino, A.L., Karner, D.B., Owens, T.L., DePaolo, D.J., 1998. Intercalibration of standards, absolute ages and uncertainties in $^{40}\text{Ar}/^{39}\text{Ar}$ dating. *Chemical Geology* 145 (1–2), 117–152.
- Salisbury, M.J., Jicha, B.R., de Silva, S.L., Singer, B.S., Jiménez, N.C., Ort, M.H., 2011. $^{40}\text{Ar}/^{39}\text{Ar}$ chronostratigraphy of Altiplano–Puna volcanic complex ignimbrites reveals the development of a major magmatic province. *Geological Society of America Bulletin* 123 (5–6), 821–840.
- Schmitt, A.K., 2011. Uranium series accessory crystal dating of magmatic processes. *Annual Reviews in Earth and Planetary Sciences* 39, 321–349.
- Schmitt, A.K., Hulen, J.B., 2008. Buried rhyolites within the active, high-temperature Salton Sea geothermal system. *Journal of Volcanology and Geothermal Research* 178 (4), 708–718.
- Schmitt, A.K., Grove, M., Harrison, T.M., Lovera, O., Hulen, J., Walters, M., 2003. The Geysers–Cobb Mountain Magma System, California (Part 1): U–Pb zircon ages of volcanic rocks, conditions of zircon crystallization and magma residence times. *Geochimica et Cosmochimica Acta* 67 (18), 3423–3442.
- Schmitt, A.K., Danišik, M., Evans, N.J., Siebel, W., Kiemle, E., Aydin, F., Harvey, J.C., 2011. Acıgöl rhyolite field, Central Anatolia (part 1): high-resolution dating of eruption episodes and zircon growth rates. *Contributions to Mineralogy and Petrology*. doi:10.1007/s00410-011-0648-x.
- Schumacher, R., Schmincke, H.-U., 1991. Internal structure and occurrence of accretionary lapilli – a case study at Laacher See Volcano. *Bulletin of Volcanology* 53 (8), 612–634.
- Schumacher, R., Mues-Schumacher, U., 1996. The Kizilkaya ignimbrite—an unusual low-aspect-ratio ignimbrite from Cappadocia, Central Turkey. *Journal of Volcanology and Geothermal Research* 70, 107–121.
- Schumacher, R., Mues-Schumacher, U., 1997. The pre-ignimbrite (phreato)plinian and phreatomagmatic phases of the Akdag–Zelve ignimbrite eruption in Central Anatolia, Turkey. *Journal of Volcanology and Geothermal Research* 78, 139–153.

- Schumacher, R., Keller, J., Bayhan, H., 1990. Depositional characteristics of ignimbrites in Cappadocia, Central Anatolia, Turkey. In: Savascin, M.Y., Eronat, A.H. (Eds.), Proc. Int. Earth Sci. Congr. on Aegean Regions, IESCA, 2, pp. 435–449.
- Şen, E., Kürkcüoğlu, B., Aydar, E., Gourgaud, A., Vincent, P.M., 2003. Volcanological evolution of Mount Erciyes stratovolcano and origin of Valibabatepe ignimbrites (Central Anatolia, Turkey). *Journal of Volcanology and Geothermal Research* 125, 225–246.
- Shane, P., 1998. Correlation of rhyolitic pyroclastic eruptive units from the Taupo volcanic zone by Fe–Ti oxide compositional data. *Bulletin of Volcanology* 60 (3), 224–238.
- Simon, J.L., Renne, P.R., Mundil, R., 2008. Implications of pre-eruptive magmatic histories of zircons for U–Pb geochronology of silicic extrusions. *Earth and Planetary Science Letters* 266 (1–2), 182–194.
- Smith, R.L., 1960. Ash flows. *Geological Society of America Bulletin* 71 (6), 796–842.
- Spell, T.L., Smith, E.J., Sanford, A., Zanetti, K.A., 2001. Systematics of xenocrystic contamination: preservation of discrete feldspar populations at McCullough Pass Caldera revealed by $^{40}\text{Ar}/^{39}\text{Ar}$ dating. *Earth and Planetary Science Letters* 190, 153–165.
- Steiger, R.H., Jäger, E., 1977. Subcommission on geochronology – convention on use of decay constants in geochronology and cosmochronology. *Earth and Planetary Science Letters* 36 (3), 359–362.
- Temel, A., 1992. Petrological and geochemical properties of Cappadocian explosive volcanism. PhD thesis, Hacettepe University, 208 pp (in Turkish).
- Temel, A., Gündoğdu, M.N., Gourgaud, A., Le Pennec, J.-L., 1998. Ignimbrites of Cappadocia (Central Anatolia, Turkey): petrology and geochemistry. *Journal of Volcanology and Geothermal Research* 85, 447–471.
- Toprak, V., Keller, J., Schumacher, R., 1994. Volcano-tectonic features of the Cappadocian volcanic province, excursion guide. International Volcanological Congress, IAVCEI, Ankara-1994, p. 58.
- Trail, D., Mojzsis, S.J., Harrison, T.M., Schmitt, A.K., Watson, E.B., Young, E.D., 2007. Constraints on Hadean zircon protoliths from oxygen isotopes, Ti-thermometry, and rare earth elements. *Geochemistry, Geophysics, Geosystems* 8. doi:10.1029/2006GC001449.
- Viereck-Götte, L., Lepetit, P., Gürel, A., Ganskow, G., Çopuroğlu, I., Abratis, M., 2010. Revised volcanostratigraphy of the Upper Miocene to Lower Pliocene Ürgüp Formation, Central Anatolian volcanic province, Turkey. In: Gropelli, G., Götte-Viereck, L. (Eds.), *Geological Society of America Special Paper* 464, pp. 85–112. doi:10.1130/2010.2464(05).
- Watson, E.B., Harrison, T.M., 1983. Zircon saturation revisited – temperature and composition effects in a variety of crustal magma types. *Earth and Planetary Science Letters* 64 (2), 295–304.
- Wilson, L., Sparks, R.S.J., Walker, G.P.L., 1980. Explosive volcanic-eruptions. 4. The control of magma properties and conduit geometry on eruption column behavior. *Geophysical Journal of the Royal Astronomical Society* 63 (1), 117–148.
- Wilson, C.J.N., Houghton, B.F., Kamp, P.J.J., McWilliams, M.O., 1995. An exceptionally widespread ignimbrite with implications for pyroclastic flow emplacement. *Nature* 378 (6557), 605–607.
- Wörner, G., Hammerschmidt, K., Henjes-Kunst, F., Lezaun, J., Wilke, H., 2000. Geochronology ($^{40}\text{Ar}/^{39}\text{Ar}$, K–Ar and He-exposure ages) of Cenozoic magmatic rocks from Northern Chile (18–22°S): implications for magmatism and tectonic evolution of the central Andes. *Revista Geologica De Chile* 27 (2), 205–240.